

**King Saud University  
College of Engineering  
Electrical Engineering Department**

# **Harmonic Reduction in the Utility Interface**

## **SCR Rectifier**

**By:**

**Turki S. Alsaleh**

**Supervised By:**

**Dr. Ali M. Eltamaly**

**January 2007**

## **Table of Contents**

Table of contents	2
Acknowledgement	3
Abstract	4

### **Chapter 1: Introduction**

1 – 1	Definition of Power Electronics	5
1 – 2	Harmonics	5
1 – 3	Three Phase Full Wave Fully Controlled Rectifier Bridge	8

### **Chapter 2: Harmonic Reduction in the Utility Interface SCR Rectifier**

2 – 1	Introduction	10
2 – 2	System Analysis	14
2 – 3	An Improved Current Injection Scheme	19

### **Chapter 3: Implementation of Boost Circuit**

3 – 1	Introduction	21
3 – 2	Control Circuit Components	22
3 – 2 – 1	DC Power Supply	22
3 – 2 – 2	Voltage Controlled Saw-tooth Oscillator and Comparator	25
3 – 2 – 3	Comparator	27
3 – 3	Power Circuit	29
3 – 4	Isolating Circuit	31
3 – 5	Simulation and Experimental Results	34
3 – 6	Conclusions	44

## **Acknowledgement**

At the outset, I thank almighty Allah for completion of this project then, I would like to express my deep gratitude and appreciation to my advisor, Dr. Ali Eltamaly for his valuable guidance, advice, patience and helpful suggestions in completing this work.

**Turki S. Alsaleh**

## **Abstract**

In this study an improved approach to reduce harmonics in the three-phase controlled rectifier are presented. The approach is based on circulating third harmonic current injection from the DC link to the utility lines to reduce utility line current harmonics in SCR converter. In the previous project (EE-498) the injection current controlled by zigzag transformer and variable R\_L\_C circuit, but in this project the resistance in the 3<sup>rd</sup> harmonic injection path has been replaced by boost converter to return the power that was dissipated in the resistor back to DC link to increase the efficiency of the system. The injection current is varied with the load current and the angle of this current also varied with the firing angle of the converter. A complete mathematical analysis, simulation results have been presented. Experimental prototype has been used to verify the mathematical and simulation results. Mathematical, simulation and experimental results show the superiority of the proposed system.



# Chapter 1

## ***INTRODUCTION***

### **1.1. Definition of Power Electronics**

Power electronics refers to control and conversion of electrical power by power semiconductor devices wherein these devices operate as switches. Advent of silicon-controlled rectifiers, abbreviated as SCRs, led to the development of a new area of application called the power electronics. Once the SCRs were available, the application area spread to many fields such as drives, power supplies, aviation electronics, high frequency inverters and power electronics originated.

Power electronics has applications that span the whole field of electrical power systems, with the power range of these applications extending from a few VA/Watts to several MVA / MW.

"Electronic power converter" is the term that is used to refer to a power electronic circuit that converts voltage and current from one form to another. These converters can be classified as:

- Rectifier converting an AC voltage to a DC voltage,
- Inverter converting a DC voltage to an AC voltage,
- Chopper or a switch-mode power supply that converts a DC voltage to another DC voltage.

### **1.2 Harmonics**

The invention of the semiconductor controlled rectifier (SCR or thyristor) in the 1950s led to increase of development new type converters, all of which are nonlinear. The major part of power system loads is in the form of nonlinear loads too much harmonics are injected to the power system. It is caused by the interaction of distorting customer loads with the impedance of supply network. Also, the increase of connecting renewable energy systems with electric utilities injects too much harmonics to the power system.

There are a number of electric devices that have nonlinear operating characteristics, and when it used in power distribution circuits it will create and generate nonlinear currents and voltages. Because of periodic non-linearity can be analyzed using the Fourier transform, these nonlinear currents and voltages have been generally referred to as "Harmonics". Also, the harmonics can be

defined as a sinusoidal component of a periodic waves or quality having frequencies that are an integral multiple of the fundamental frequency.

Among the devices that can generate nonlinear currents transformers and induction machines (Because of magnetic core saturation) and power electronics assemblies.

The electric utilities recognized the importance of harmonics as early as the 1930's such behavior is viewed as a potentially growing concern in modern power distribution network.

Harmonics standards and limits evolved to give a standard level of harmonics can be injected to the power system from any power system component. The first standard (EN50006) by European Committee for Electro-technical Standardization (CENELEC) that was developed by 14th European committee. Many other standardizations were done and are listed in IEC61000-3-4, 1998.

The IEEE standard 519-1992 is a recommended practice for power factor correction and harmonic impact limitation for static power converters. It is convenient to employ a set of analysis tools known as Fourier transform in the analysis of the distorted waveforms. In general, a non-sinusoidal waveform  $f(t)$  repeating with an angular frequency  $\omega$  can be expressed as in the following equation.

$$f(t) = a_0 + \sum_{n=1}^{\infty} (a_n \cos(n\omega t) + b_n \sin(n\omega t)) \quad (1.1)$$

$$\text{where } a_n = \frac{1}{\pi} \int_0^{2\pi} f(t) \cos(n\omega t) d\omega t \quad (1.2)$$

$$\text{and } b_n = \frac{1}{\pi} \int_0^{2\pi} f(t) \sin(n\omega t) d\omega t \quad (1.3)$$

Each frequency component  $n$  has the following value

$$f_n(t) = a_n \cos(n\omega t) + b_n \sin(n\omega t) \quad (1.4)$$

$f_n(t)$  can be represented as a phasor in terms of its *rms* value as shown in the following equation

$$F_n = \sqrt{\frac{a_n^2 + b_n^2}{2}} e^{j\varphi_n} \quad (1.5)$$

$$\text{Where } \varphi_n = \tan^{-1} \frac{-b_n}{a_n} \quad (1.6)$$

The amount of distortion in the voltage or current waveform is qualified by means of an Total Harmonic Distortion (THD). The THD in current and voltage are given as shown in (1.7) and (1.8) respectively.

$$THD_i = 100 * \frac{\sqrt{I_s^2 - I_{s1}^2}}{I_{s1}} = 100 * \frac{\sqrt{\sum_{n \neq 1} I_{sn}^2}}{I_{s1}} \quad (1.7)$$

$$THD_v = 100 * \frac{\sqrt{V_s^2 - V_{s1}^2}}{V_{s1}} = 100 * \frac{\sqrt{\sum_{n \neq 1} V_{sn}^2}}{V_{s1}} \quad (1.8)$$

Where  $THD_i$  &  $THD_v$  are the Total Harmonic Distortion in the current and voltage waveforms respectively.

Current and voltage limitations included in the update IEEE 519 1992 are shown in Table(1.1) and Table(1.2) respectively.

Table (1.1) IEEE 519-1992 current distortion limits for general distribution systems  
(120 to 69kV) the maximum harmonic current distortion in percent of  $I_L$

Individual Harmonic order (Odd Harmonics)						
$I_{SC} / I_L$	$n < 11$	$11 \leq n < 17$	$17 \leq n < 23$	$23 \leq n < 35$	$35 \leq n < \infty$	THD
$< 20$	4.0	2.0	1.5	0.6	0.3	5.0
$20 < 50$	7.0	3.5	2.5	1.0	0.5	8.0
$50 < 100$	10.0	4.5	4.0	1.5	0.7	12.0
$100 < 1000$	12.0	5.5	5.0	2.0	1.0	15.0
$> 1000$	15.0	7.0	6.0	2.5	1.4	20.0

Where; THD as shown in (1.7).

$I_{SC}$  is the maximum short-circuit current at the point of common coupling (PCC).

$I_L$  is the maximum demand load current at the point of common coupling (PCC).

Table (1.2) Voltage distortion limits

Bus voltage at PCC	Individual voltage distortion (%)	$THD_v$ (%)
69 kV and below	3.0	5.0
69.001 kV through 161kV	1.5	2.5
161.001kV and above	1	1.5

### 1.3 Three Phase Full Wave Fully Controlled Rectifier Bridge:

Three-phase full wave controlled rectifier shown in Fig.1.1. As we can see in this figure the thyristors has labels T1, T2,.....,T6. The label of each thyristor is chosen to be identical to triggering sequence where thyristors are triggered in the sequence of T1, T2,.....,T6 which is clear from the thyristors currents shown in Fig.1.2.

Three-phase full wave-fully controlled rectifier with pure *DC* load current is shown in Fig.1.1. Fig.1.2 shows various currents and voltage of the converter shown in Fig.1.1 when the delay angle is less than  $60^\circ$ . As we see in Fig.1.2, the load voltage is only positive and there is no negative period in the output waveform. Fig.1.3 shows FFT components of output voltage of rectifier shown in Fig.1.1 for  $\alpha < 60^\circ$ .

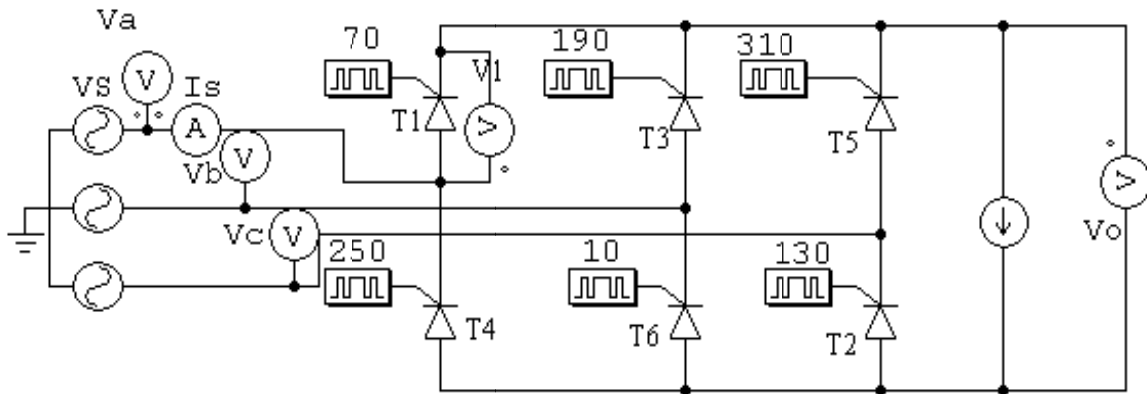


Fig.1.1 Three phase full wave fully controlled rectifier with pure *dc* load current

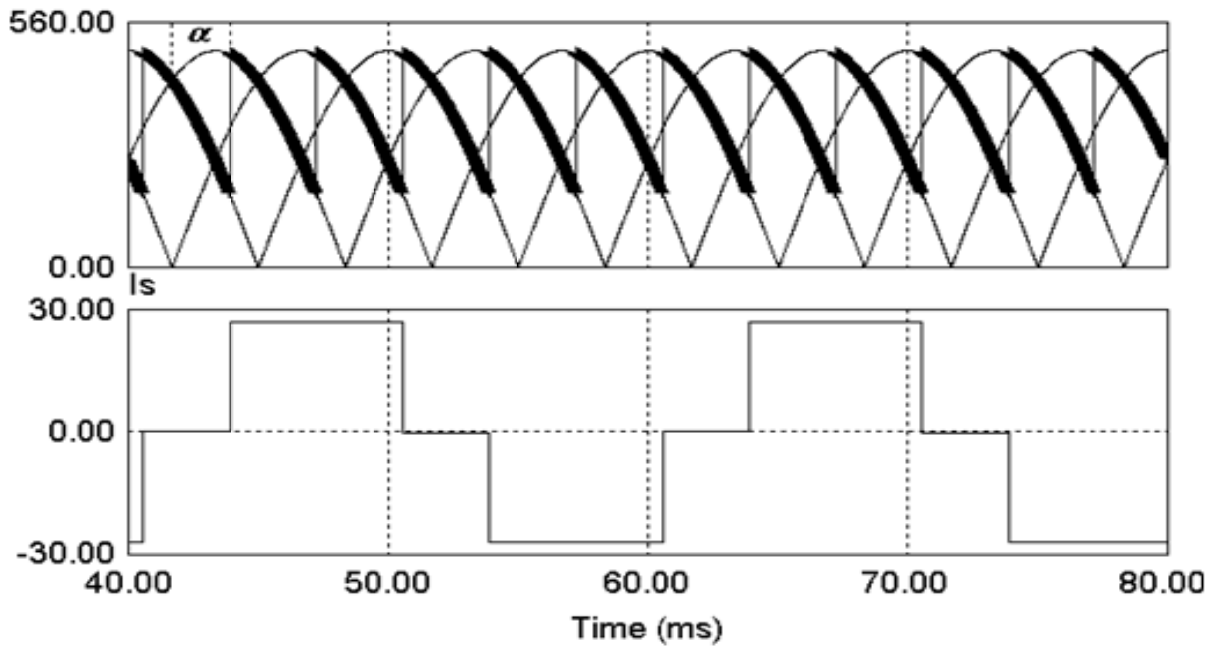


Fig.1.2 Output voltage and supply current waveforms along with three phase line voltages for the rectifier shown in Fig.1.1 for  $\alpha < 60^\circ$  with pure DC current load.

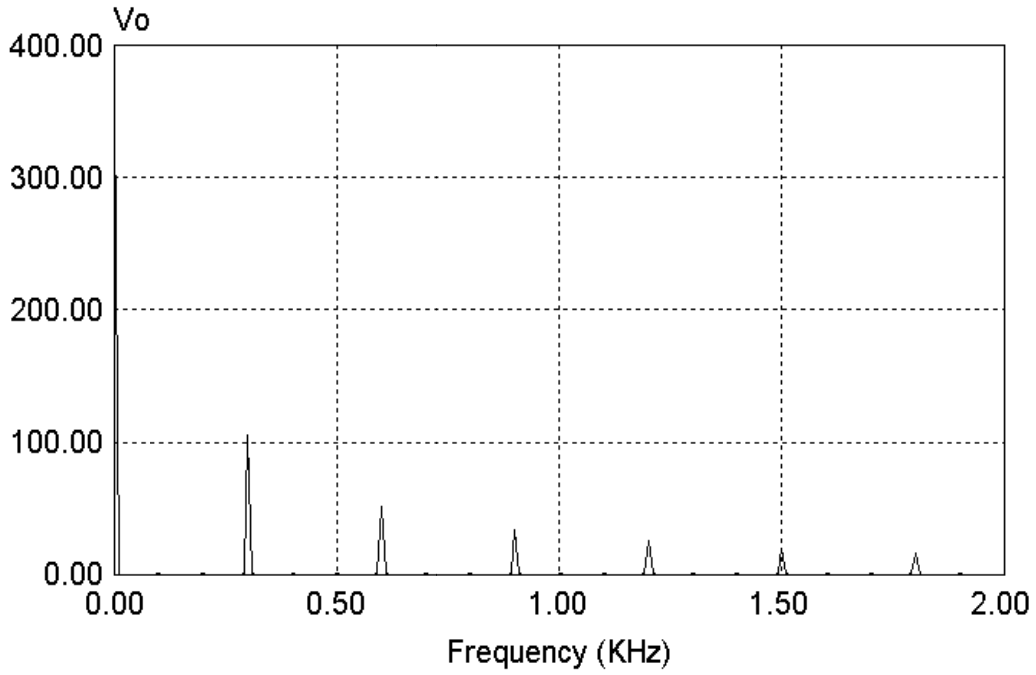


Fig.1.3 FFT components of SCR, secondary, primary currents respectively of rectifier shown in Fig.1.1

$$V_{dc} = \frac{3}{\pi} \int_{\pi/6+\alpha}^{\pi/2+\alpha} \sqrt{3} V_m \sin(\omega t + \frac{\pi}{6}) d\omega t = \frac{3\sqrt{3} V_m}{\pi} \cos \alpha \quad (1.9)$$

The maximum average output voltage for delay angle  $\alpha=0$  is

$$V_{dm} = \frac{3\sqrt{3} V_m}{\pi} \quad (1.10)$$

The normalized average output voltage is as shown in (1.20)

$$V_n = \frac{V_{dc}}{V_{dm}} = \cos \alpha \quad (1.11)$$

The *rms* value of the output voltage is found from the following equation:

$$V_{rms} = \sqrt{\frac{3}{\pi} \int_{\pi/6+\alpha}^{\pi/2+\alpha} 3 \left( V_m \sin(\omega t + \frac{\pi}{6}) \right)^2 d\omega t} = \sqrt{3} V_m \sqrt{\left( \frac{1}{2} + \frac{3\sqrt{3}}{4\pi} \cos 2\alpha \right)} \quad (1.12)$$

## Chapter 2

# HARMONIC REDUCTION IN THE UTILITY INTERFACE SCR RECTIFIER

### 2.1 Introduction

The line commutated SCR rectifier is reliable and easily scalable to higher voltage/ power ratings. Fig.2.1 (a).shows a line commutated SCR rectifier employed as a utility interface. The utility line current and its FFT are shown in Fig.2.2(b).This wave-shape described by the following series.

$$i(\omega t) = \frac{2\sqrt{3}}{\pi} I_o \left( \cos \omega t - \frac{1}{5} \cos (5\omega t) - \frac{1}{7} \cos (7\omega t) + \frac{1}{11} \cos (11\omega t) + \frac{1}{13} \cos (13\omega t) \dots \right) \quad (2.1)$$

Where  $i(t)$  is the instantaneous line current and  $I_o$  is the DC current

Therefore the line current contains components at  $5\omega t$ ,  $7\omega t$ ,  $11\omega t$ ,  $13\omega t$  etc. These are so called characteristics harmonics of the three-phase six-pulse bridge. From (2.1) the THD for this waveform is about 35%. This current waveform presents high harmonics and contributes to many ill effects to the electric utility.

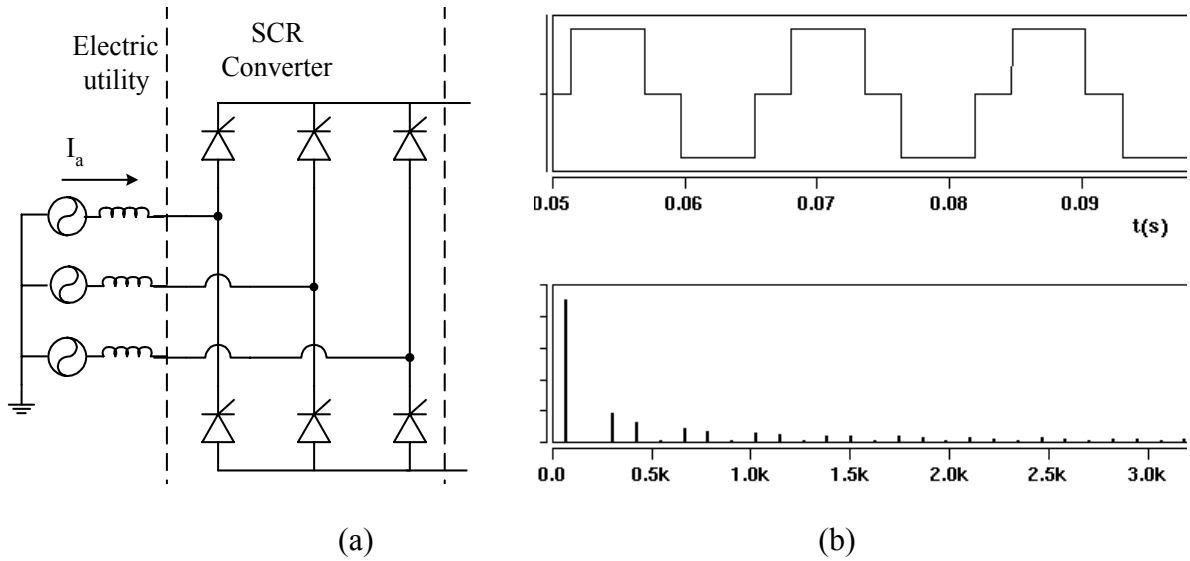


Fig.2.1 SCR converter without 3<sup>rd</sup> harmonic injection and utility line current.

Many researches have been done to reduce the harmonic contents in utility line currents like increase the pulse numbers of utility line currents or by injection technique. Twelve-pulse bridge connection is the most widely used in high number of pulses operation. Twelve-pulse technique is using in most HVDC schemes and in very large variable speed drives for DC and AC motors as well as in renewable energy system. An example of twelve-pulse bridge is shown in Fig.2.2. In fact any combination such as this which gives a 30°-phase shift will form a twelve-pulse converter. In

## Chapter 2

# HARMONIC REDUCTION IN THE UTILITY INTERFACE SCR RECTIFIER

### 2.1 Introduction

The line commutated SCR rectifier is reliable and easily scalable to higher voltage/ power ratings. Fig.2.1 (a).shows a line commutated SCR rectifier employed as a utility interface. The utility line current and its FFT are shown in Fig.2.2(b).This wave-shape described by the following series.

$$i(\omega t) = \frac{2\sqrt{3}}{\pi} I_o \left( \cos \omega t - \frac{1}{5} \cos (5\omega t) - \frac{1}{7} \cos (7\omega t) + \frac{1}{11} \cos (11\omega t) + \frac{1}{13} \cos (13\omega t) \dots \right) \quad (2.1)$$

Where  $i(t)$  is the instantaneous line current and  $I_o$  is the DC current

Therefore the line current contains components at  $5\omega t$ ,  $7\omega t$ ,  $11\omega t$ ,  $13\omega t$  etc. These are so called characteristics harmonics of the three-phase six-pulse bridge. From (2.1) the THD for this waveform is about 35%. This current waveform presents high harmonics and contributes to many ill effects to the electric utility.

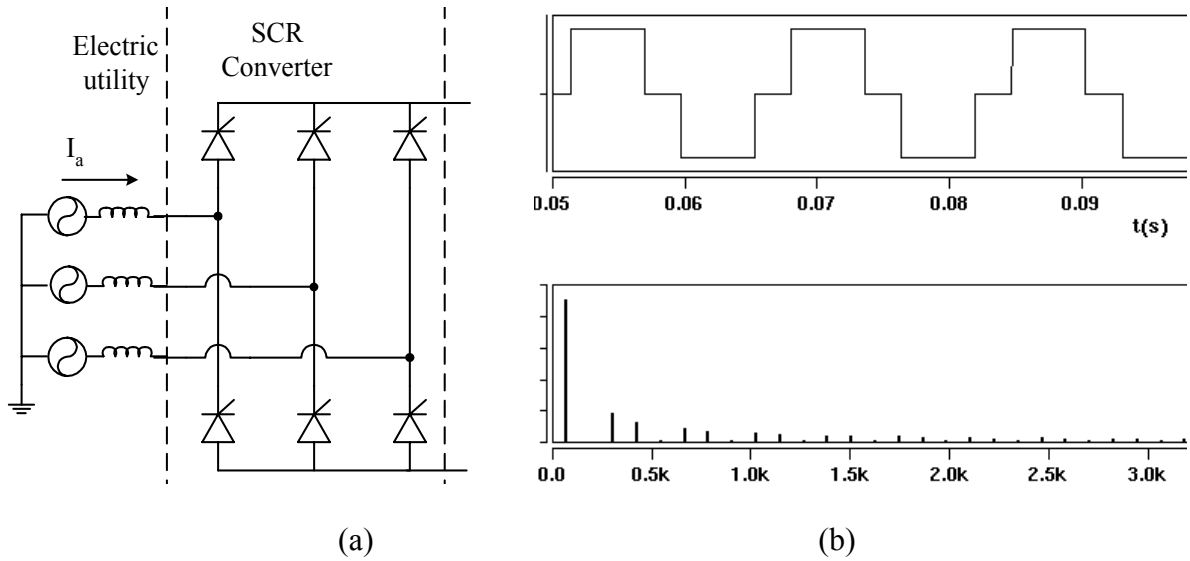


Fig.2.1 SCR converter without 3<sup>rd</sup> harmonic injection and utility line current.

Many researches have been done to reduce the harmonic contents in utility line currents like increase the pulse numbers of utility line currents or by injection technique. Twelve-pulse bridge connection is the most widely used in high number of pulses operation. Twelve-pulse technique is using in most HVDC schemes and in very large variable speed drives for DC and AC motors as well as in renewable energy system. An example of twelve-pulse bridge is shown in Fig.2.2. In fact any combination such as this which gives a 30°-phase shift will form a twelve-pulse converter. In

this kind of converters, each converter will generate all kind of harmonics described above but some will cancel, being equal in amplitude but 180° out of phase. This happened to 5<sup>th</sup> and 7<sup>th</sup> harmonics along with some of higher order components. An analysis of the waveform shows that the AC line current can be described by:

$$i(\omega t) = \frac{2\sqrt{3}}{\pi} I_d \left( \cos(\omega t) - \frac{1}{11} \cos(5\omega t) + \frac{1}{13} \cos(13\omega t) - \frac{1}{23} \cos(23\omega t) + \frac{1}{25} \cos(25\omega t) \right) \quad (2.2)$$

As shown in (2.2) the THD<sub>i</sub> is about 13.5%. The waveform of utility line current is shown in Fig.2.3. Higher pulse number like 18-pulse or 24-pulse reduces the THD more and more but its applications very rare. In all kind of higher pulse number the converter needs special transformer. Sometimes the transformers required are complex, expensive and it will not be ready available from manufacturer.

The main idea here is to use a six-pulse bridge directly to three-phase supply without transformer. But the THD must be lower than the IEEE-519 1992 limits.

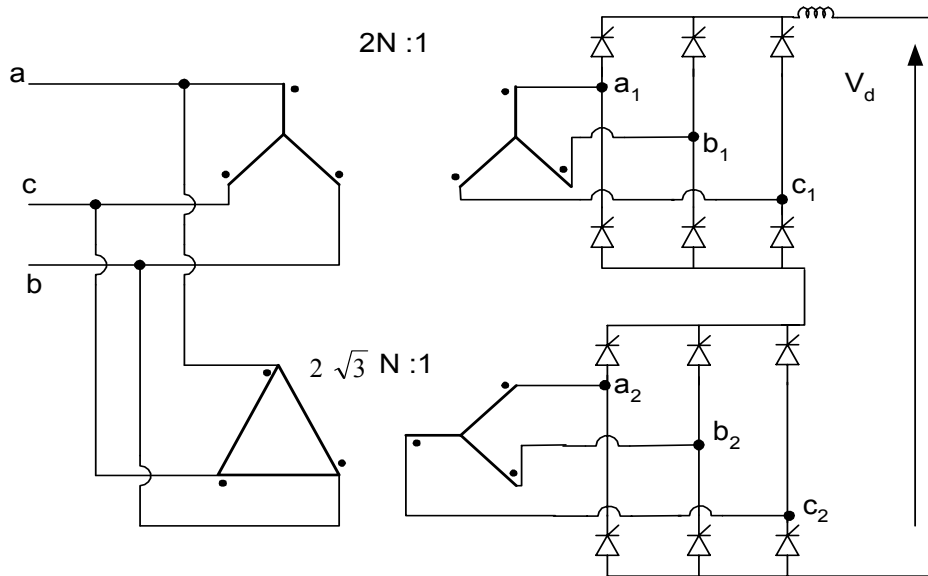
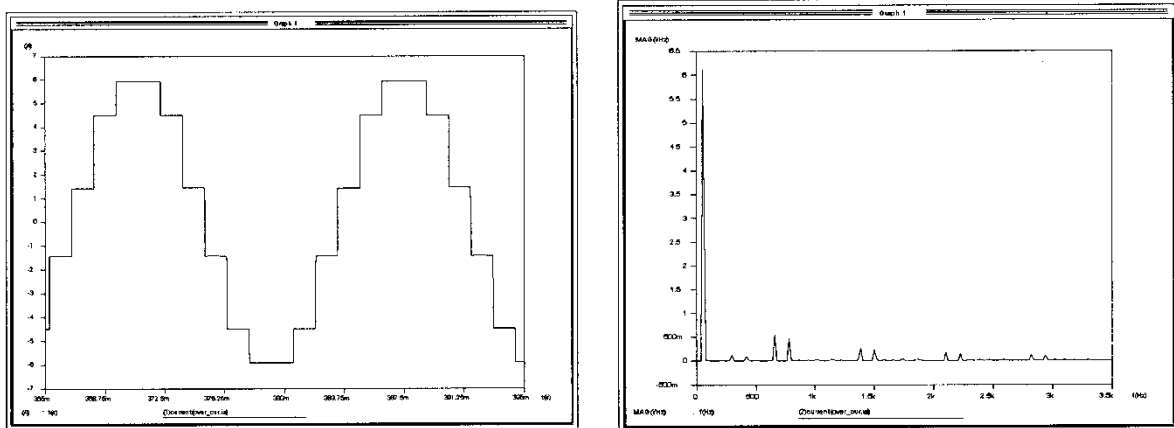


Fig.2.2 Twelve-pulse converter arrangement



(a) Utility input current.

(b) FFT components of utility current.

Fig.2.3 Simulation results of 12-pulse system.



In order to minimize harmonics generated by SCR rectifier, Fig.2.4 shows a third harmonic current injection scheme to reduce utility current THD. This scheme suffers from the following disadvantages:

- It requires an Y /  $\Delta$  input isolation transformer which increases the total system cost.
- Two IGBTs on the DC side are in the series path of the power flow.
- The DC link voltage is higher than nominal and warrants re-design of the inverter stage.
- Suffer from increased losses.

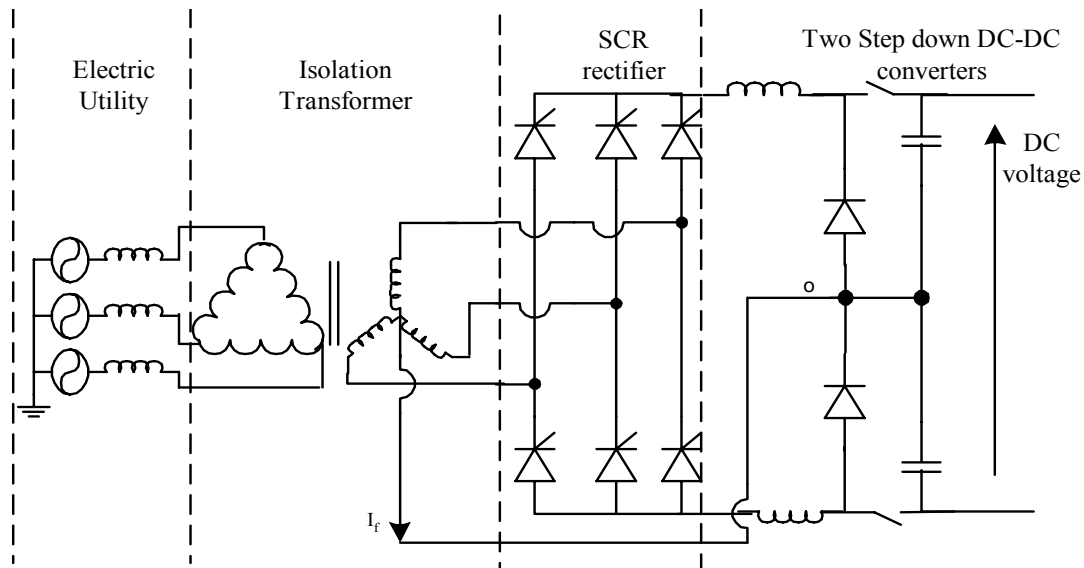


Fig.2.4 Harmonic reduction in SCR rectifier type utility interface using two step down DC-DC converters.

Fig.2.5 shows another injection of third harmonic current  $I_f$  technique for utility interface of WTG using SCR converter. A tuned LC branch connected in star is employed to provide the neutral. This scheme suffers from the following disadvantages:

- (i).The LC branches are bulky and draw reactive power of fundamental frequency.
- (ii).The LC branch can resonate with other element in the electric utility.
- (iii).The current in the reinjection branch is very sensitive to the deviation of L and C values.
- (iv).This technique does not take into account the harmonic level in the DC-link current.

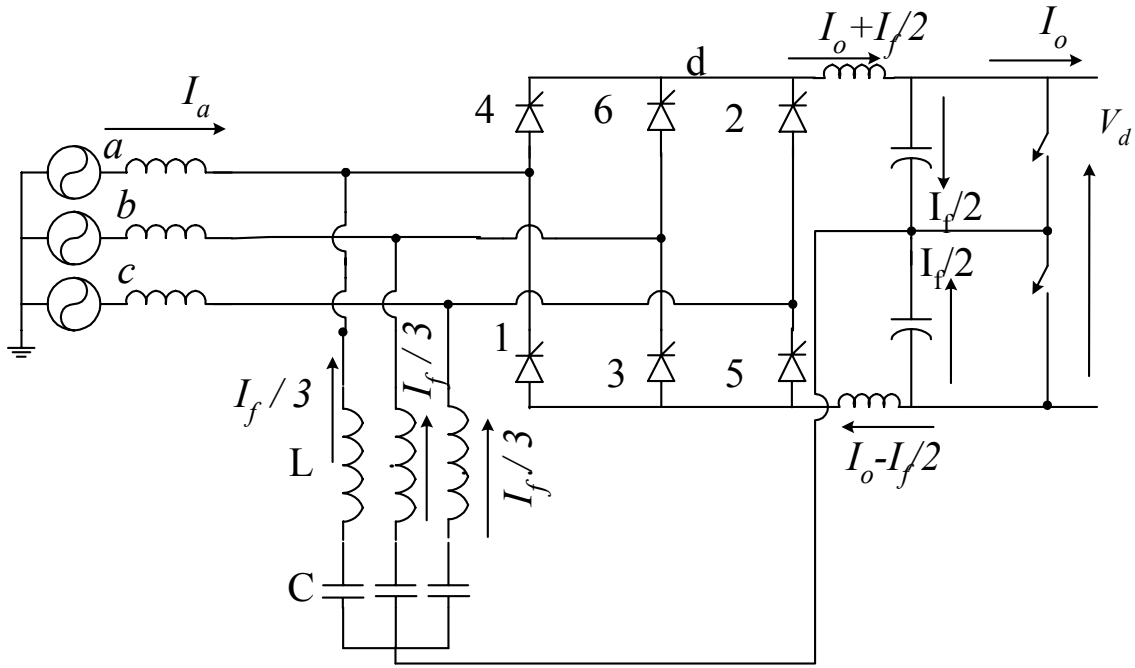
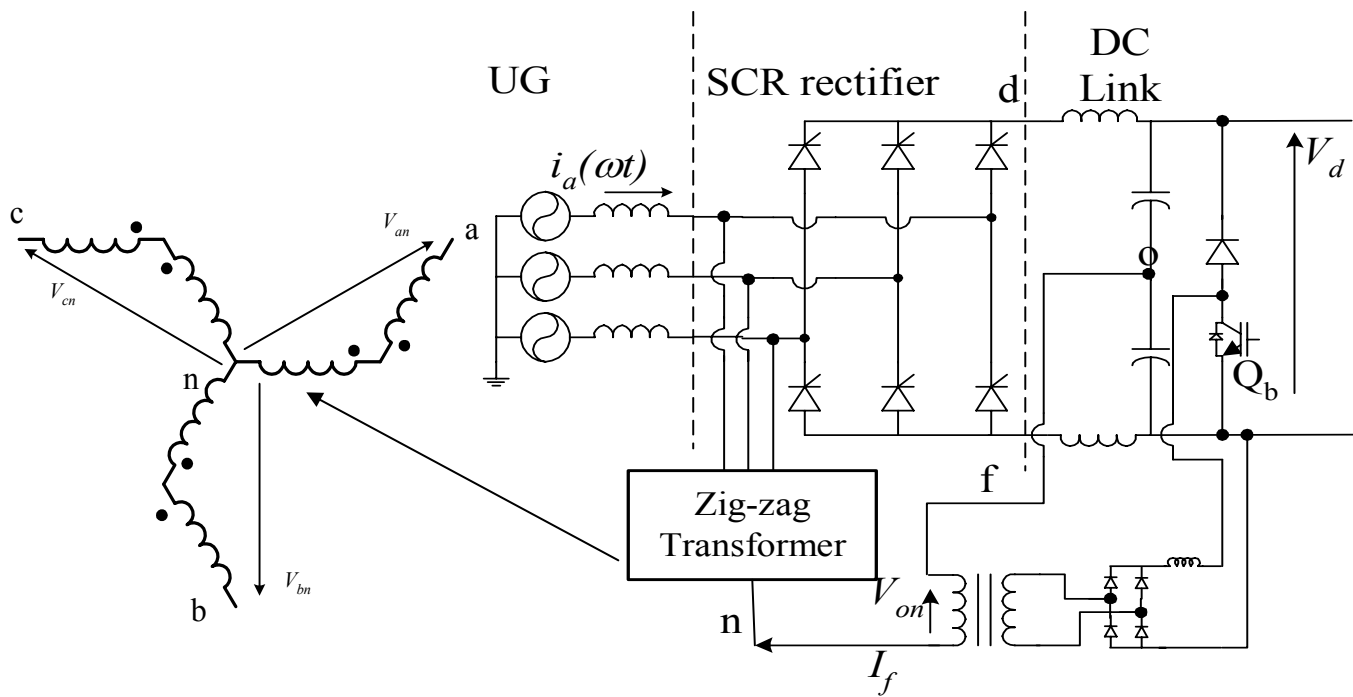


Fig.2.5 The injection technique using three-LC branches.

Another harmonic reduction scheme is shown in Fig.2.6. This scheme consists of zig/zag transformer, single-phase transformer connected between the DC-link mid-point 'o' and the zig/zag transformer neutral 'n'. The secondary of single-phase transformer is connected to a rectifier, boost converter stage feeding the DC-link. By operating the single switch ( $Q_b$ ), the injected current shape  $I_f$  can be regulated and reduction in utility line current harmonics can be achieved. The controllable single switch boost converter ( $Q_b$ ) connected in shunt regulates the utility line current harmonics against load variations. The boost converter is controlled to emulate a loss less resistor by returning power back to DC-link. The zig/zag transformer exhibits high magnetizing impedance for fundamental frequency voltages and very low leakage for third harmonics (zero sequence current). Also, the zig/zag transformer creates a neutral point to circulate the injection current from DC to line currents.

In Fig.2.6 a shape for injected current is derived, such that utility line current shape is sinusoidal. A controllable single switch boost converter connected in shunt regulates the injected current against load variations. The proposed approach has the following advantages:

- (i) It can be applied to line commutated SCR rectifier or SCR inverter.
- (ii) No additional components in the path of power flow.
- (iii) A single switch boost converter connected in shunt is sufficient to inject the circulating current  $I_f$ .
- (iv) The utility line current is near sinusoidal in shape under varying load conditions.
- (v) The proposed approach can be viewed as an add-on option.



## 2.2 System Analysis

In this section a thoroughly analysis of the SCR rectifier output line currents and principles of harmonic current cancellation by the proposed harmonic current injection is presented. To facilitate this analysis we will assume the voltage drops across the forward thyristors are negligible. The operation can be divided into six switching states as shown in Fig.2.7 to Fig.2.12. In each state pair of thyristors are on and indicated in bold style to identify on ones. The path of circulating third harmonic current, DC-link current and electric utility line currents are indicated in each state.

By inspecting the current of phase (a) in Fig.2.7 to Fig.2.12 we can see that:

- $I_a = -I_f/3$  in **state-1** and **state-4**.
- $I_a = I_o + I_f/6$  in **state-2** and **state-3**.
- $I_a = -I_o + I_f/6$  in **state-5** and **state-6**.

where  $I_f$  : Total injection current and  $I_o$  is the DC-link current.

It is clear that the line current  $I_a$  of phase ( $a$ ) is altered in shape with the 3<sup>rd</sup> harmonic injection current and in order to represent this current mathematically, switching functions  $SW_1, SW_2, SW_3$  are designed and are shown in Fig 2.13. The utility line currents of phase ( $a$ ) of SCR converter can be expressed in terms of  $I_o, I_f$  and the switching functions  $SW_1, SW_2, \text{ and } SW_3$  as in the following equation (See Fig.2.13):

$$I_a(\omega t) = \frac{I_f(\omega t)}{3} SW_1(\omega t) + \frac{I_f(\omega t)}{6} SW_3(\omega t) + SW_2(\omega t) I_o \quad (2.3)$$

By simplifying (2.3), we can obtain the following equation:

$$I_a(\omega t) = \frac{I_f(\omega t)}{3} \left[ SW_1(\omega t) + \frac{SW_3(\omega t)}{2} \right] + SW_2(\omega t)I_o \quad (2.4)$$

Where  $I_a(\omega t)$  is the AC line current of phase ( $a$ )

The current in (2.4) is shown in Fig.2.13. The resultant utility line current is altered and becomes near sinusoidal in shape. Injection current shape for  $I_f$  is derived in order to drastically improve the quality of  $I_a$ .

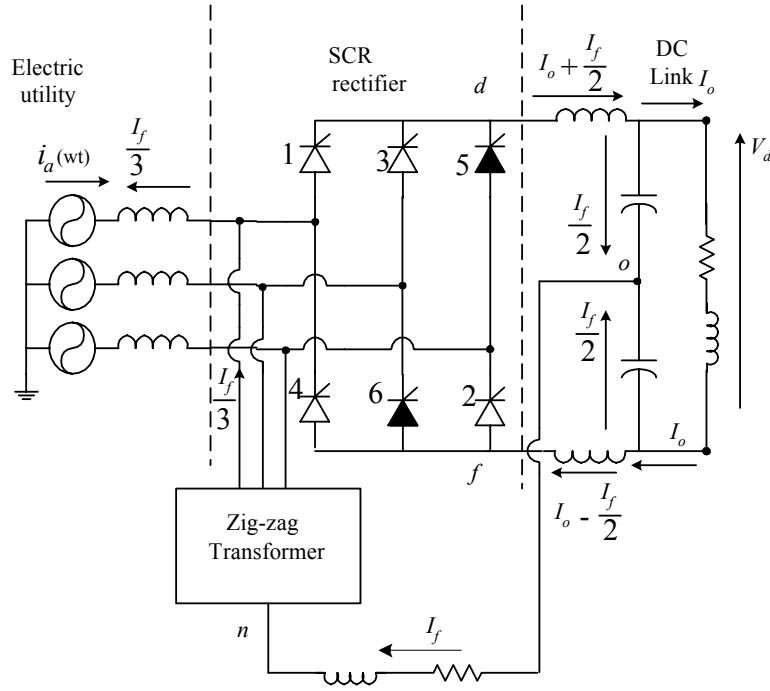


Fig.2.7 State-1 SCR<sub>5</sub> and SCR<sub>6</sub> are on.

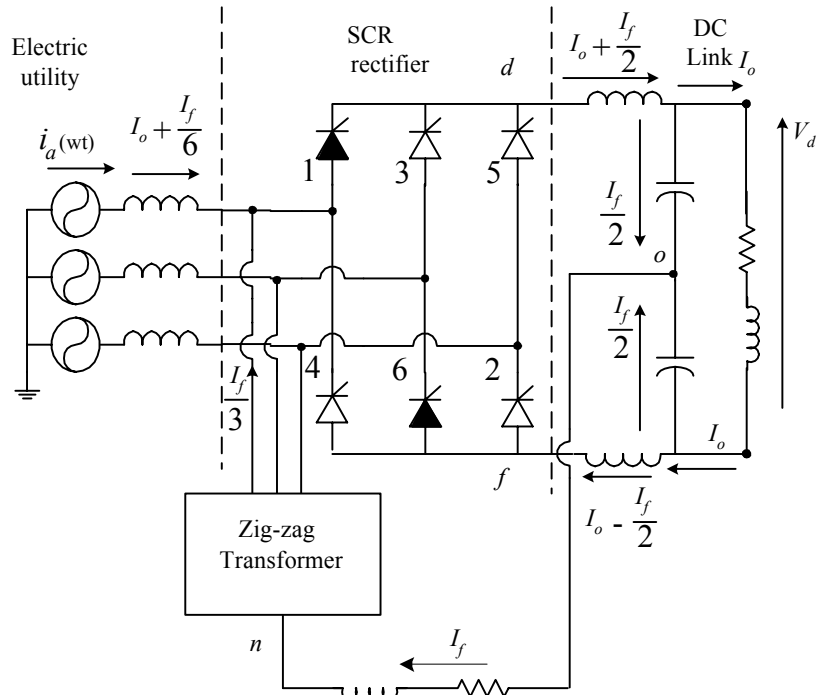
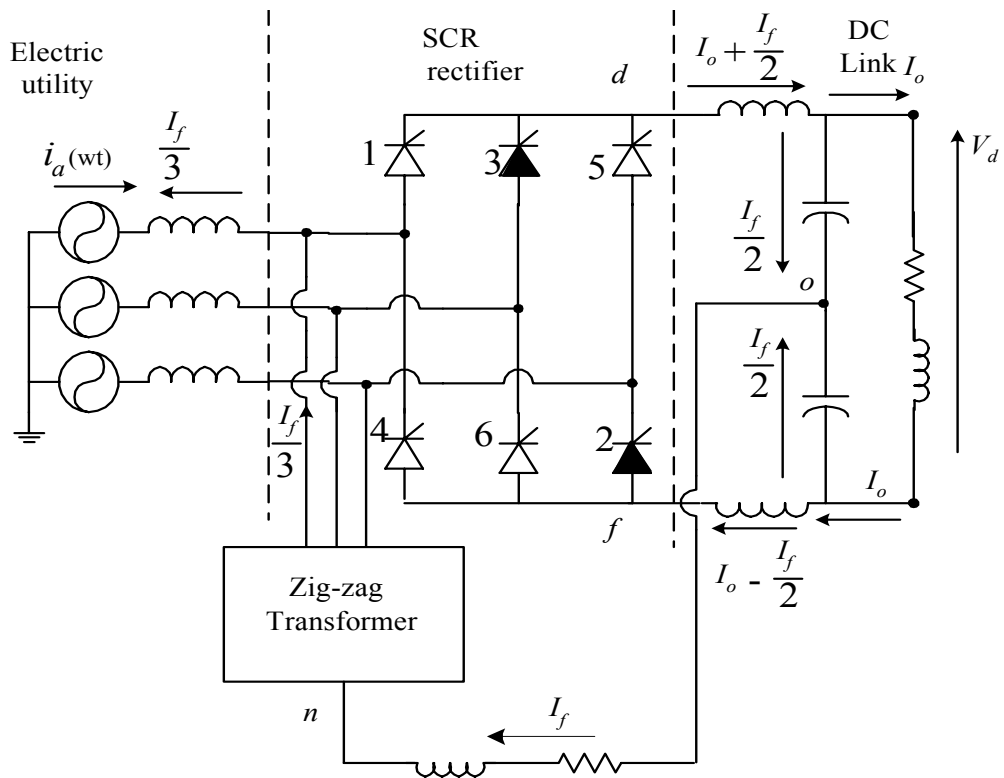
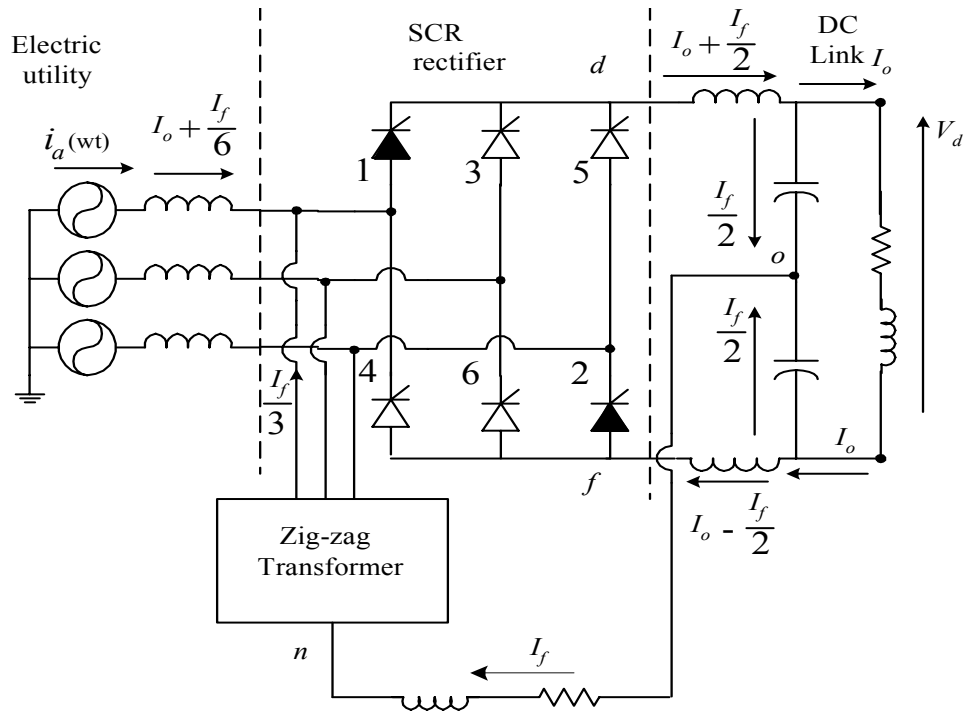


Fig.2.8 State-2 SCR<sub>1</sub> and SCR<sub>6</sub> are on.



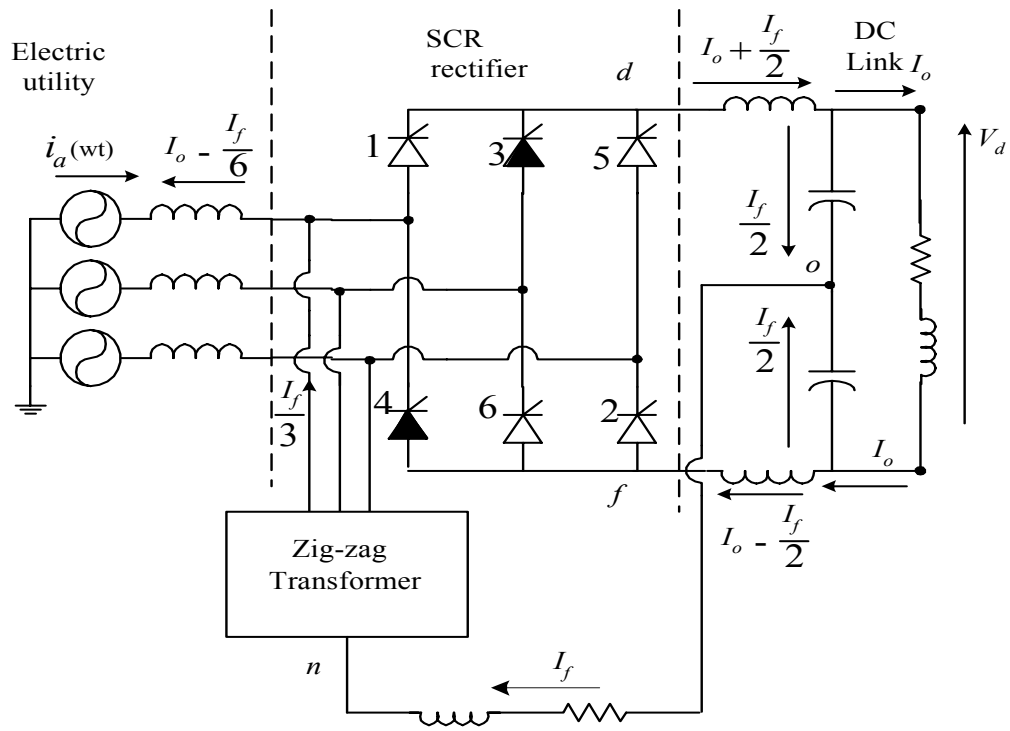


Fig.2.11 State-5 SCR<sub>3</sub> and SCR<sub>4</sub> are on.

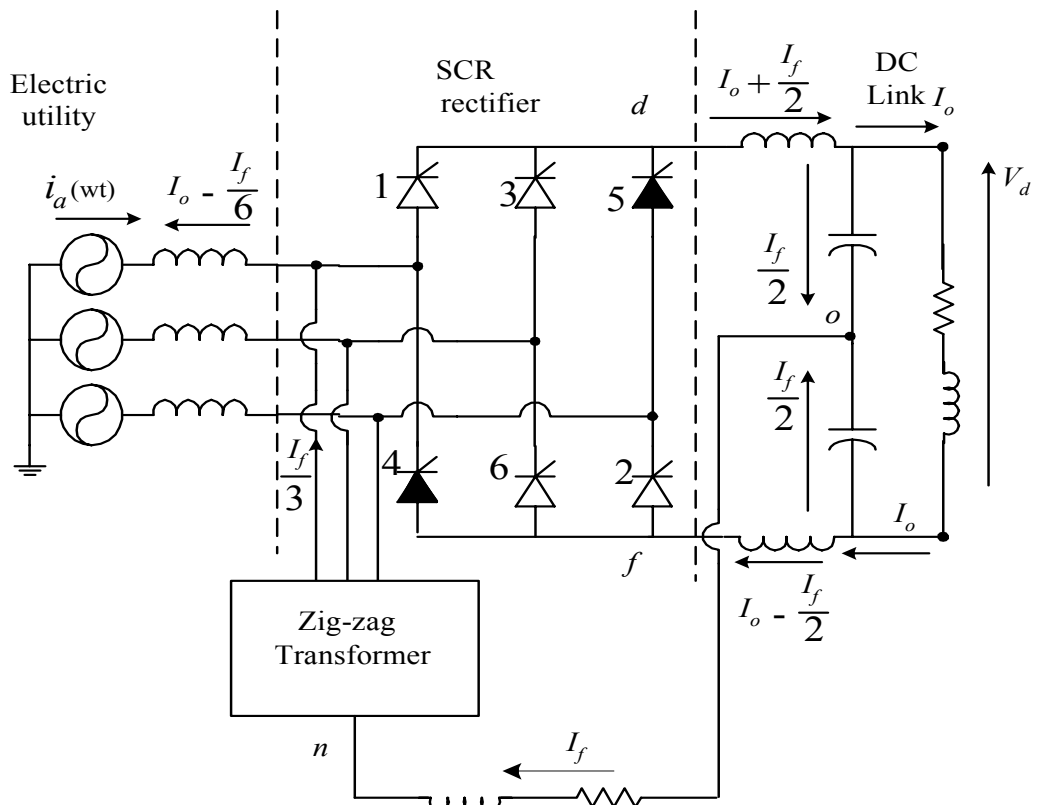


Fig.2.12 State-6, SCR<sub>4</sub> and SCR<sub>5</sub> are on.

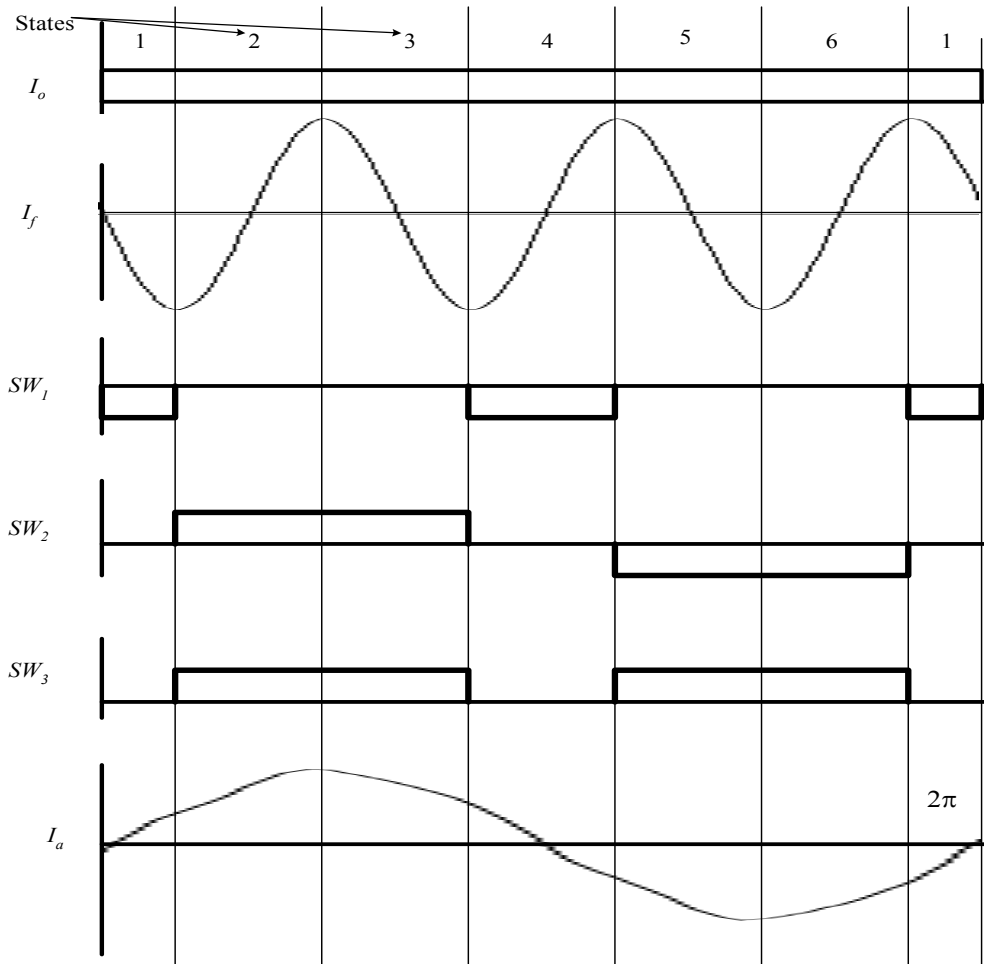


Fig.2.13 Waveforms of  $I_o$ ,  $I_f$ ,  $SW_1$ ,  $SW_2$ ,  $SW_3$  and  $I_a$  derived from switching states.

The relationship between the utility line current  $i_a(\omega t)$ , injected current  $i_f(\omega t)$  and DC-Link current  $i_o(\omega t)$  is given in (2.4) and Fig.2.13. This current became more sinusoidal and using the injection technique reduces total harmonic distortion. It is clear from Fig.2.13 and (2.4) that for a given load current  $i_o(\omega t)$  a proper choice of  $I_f$  would minimize the THD of input current. The Fourier series of  $SW_1$ ,  $SW_2$  and  $SW_3$  (Fig.2.13) can be written as in (2.5), (2.6) and (2.7).

$$SW_1(\omega t) = -\frac{1}{3} + \frac{2\sqrt{3}}{\pi} * \left( -\frac{\cos(2\omega t)}{2} - \frac{\cos(4\omega t)}{4} + \frac{\cos(8\omega t)}{8} + \frac{\cos(10\omega t)}{10} - \frac{\cos(14\omega t)}{14} - \frac{\cos(16\omega t)}{16} + \dots \right) \quad (2.5)$$

$$SW_2(\omega t) = \frac{2\sqrt{3}}{\pi} * \left( \sin(\omega t) - \frac{\sin(5\omega t)}{5} - \frac{\sin(7\omega t)}{7} + \frac{\sin(11\omega t)}{11} + \frac{\sin(13\omega t)}{13} - \frac{\sin(17\omega t)}{17} - \frac{\sin(19\omega t)}{19} + \dots \right) \quad (2.6)$$

$$SW_3(\omega t) = \frac{2}{3} + \frac{2\sqrt{3}}{\pi} * \left( -\frac{\cos(2\omega t)}{2} - \frac{\cos(4\omega t)}{4} + \frac{\cos(8\omega t)}{8} + \frac{\cos(10\omega t)}{10} - \frac{\cos(14\omega t)}{14} - \frac{\cos(16\omega t)}{16} + \dots \right) \quad (2.7)$$

Fig.2.14 shows the results of 3<sup>rd</sup> harmonic current  $I_f$  and the shape of  $i_a(\omega t)$  at  $I_f = I_o$ . It can be seen that the utility line current shape is not pure sine wave. In case of higher harmonic contents in the DC-link current, the THD of utility line current will be higher. For this reason, we have to modify the injection current to generate pure sine-wave utility line current for any level of harmonic contents in DC-link current. In the new proposed technique the utility line current will be more sinusoidal in shape by changing the shape of injection current.

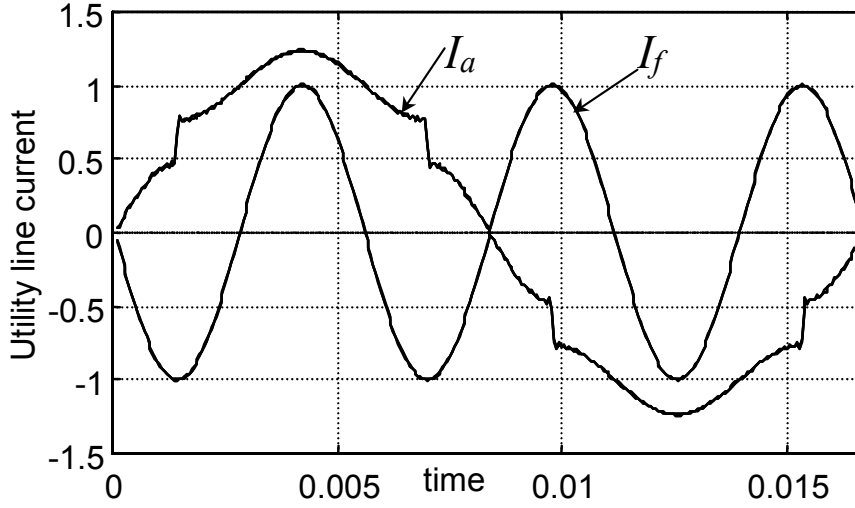


Fig.2.14 Utility line current and 3<sup>rd</sup> harmonic injection current at  $I_f=I_o$ .

### 2.3 An Improved Current Injection Scheme.

In this section an improved shape for injection current is derived to achieve sinusoidal line current in the presence of DC-link current ripple. From (2.4) we have the following equation for  $i_f(\omega t)$ :

$$i_f(\omega t) = \frac{i_a(\omega t) - SW_2(\omega t)i_o(\omega t)}{\frac{1}{3} * \left[ SW_1(\omega t) + \frac{SW_3(\omega t)}{2} \right]} \quad (2.8)$$

By forcing the utility line current  $i_a(\omega t)$  in (2.8) to be sinusoidal; the required shape for the injection current  $i_f(\omega t)$  can be obtained. In this case, zero THD in the utility line current can be achieved for any harmonic level in DC-link current. The injection current shape can be calculated for pure DC-link current. The DC-link inductor has been assumed to be high and the DC-link current ripples is negligible as shown in (2.9).

$$i_o(\omega t) = I_o \quad (2.9)$$

Substituting (2.5), (2.6), (2.7) and (2.9) into (2.8) and forcing the utility line current  $i_a(\omega t)$  to sinusoidal with fundamental component amplitude yields:

$$\frac{i_f(\omega t)}{I_o} = \frac{\sqrt{2} * \left[ -\frac{\sin(5\omega t)}{5} - \frac{\sin(7\omega t)}{7} + \frac{\sin(11\omega t)}{11} + \frac{\sin(13\omega t)}{13} \right]}{\left[ -\frac{\cos(2\omega t)}{2} - \frac{\cos(4\omega t)}{4} + \frac{\cos(8\omega t)}{8} + \frac{\cos(10\omega t)}{10} \right]} \quad (2.10)$$

From (2.10), the new shape of injection current can be drawn as shown in Fig.2.15. Therefore, by injecting the current  $i_f(\omega t)$  as shown in Fig.2.15, sinusoidal utility line current is obtained. Fig.2.16 shows the utility line current  $i_a(\omega t)$  as a result of injected current  $i_f(\omega t)$  shown in Fig.2.15. It is clear that  $i_a(\omega t)$  is near sinusoidal and is of much higher quality compared to Fig.2.14. The THD of waveform in Fig.2.16 is less than 1% and it is easy to achieve the requirements of IEC 61000-3-4, 1998 standardization. Fig.2.17 shows the voltage  $V_{dn}$ ,  $V_{fn}$ , and  $V_{on}$ .



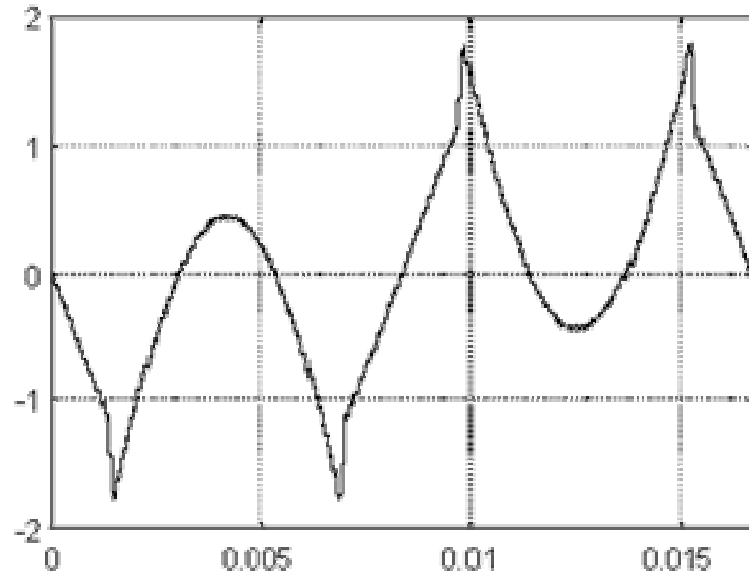


Fig.2.15 New injection current shape for a complete one period

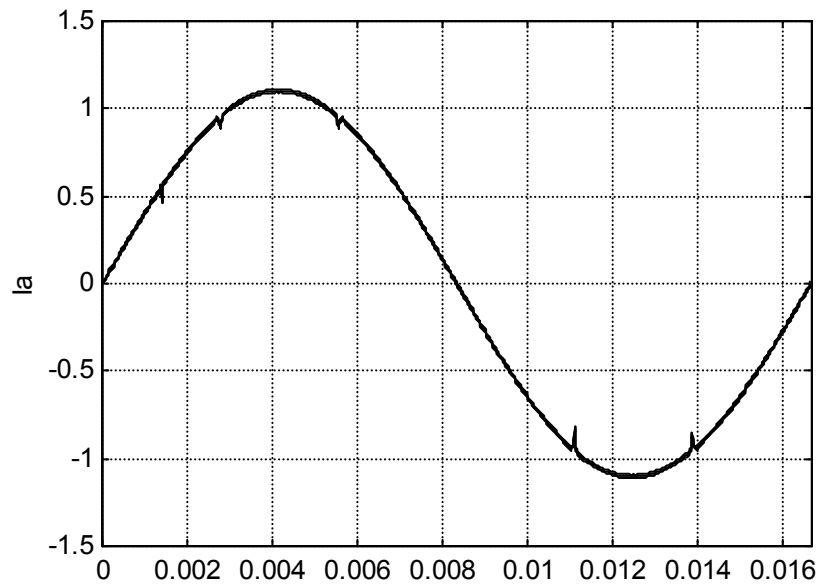


Fig.2.16 Utility line current  $i_a(\omega t)/I_o$

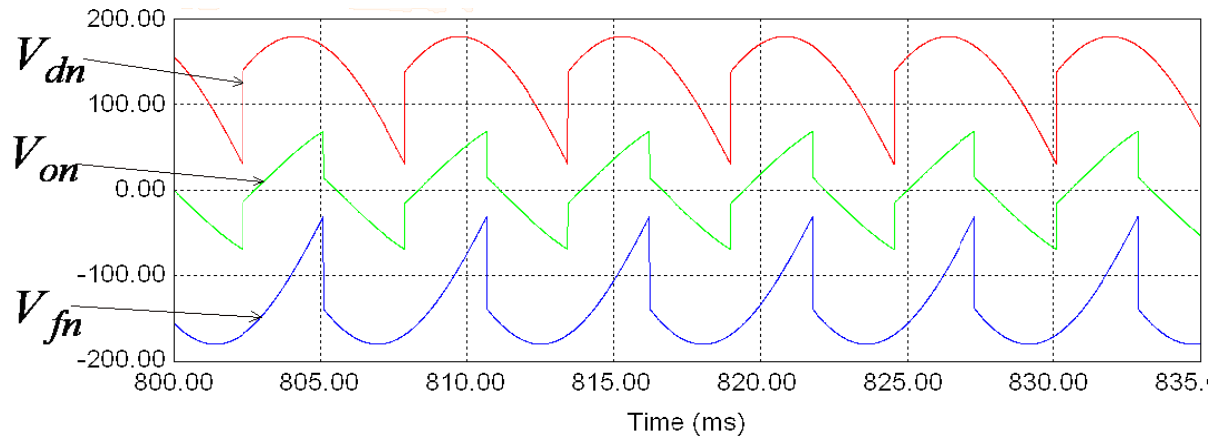


Fig.2.17 The voltages in SCR rectifier, (V)  $V_{dn}$  is The voltage between point 'd' and 'n',  $V_{fn}$  is The voltage between point 'f' and 'n' and  $V_{on}$  is The voltage between point 'o' and 'n'

## Chapter3

### ***IMPLEMENTATION OF BOOST CIRCUIT***

#### **3-1 Introduction**

The boost or step-up converter has an output voltage that is always greater than the input voltage.

Fig.3.1 shows a conceptual diagram of boost converter. The basic operation mechanism is that when the switch is closed the load is isolated from the input by the diode, and current builds up in the inductor. This current build is effectively storing energy in the field of the inductor. When the switch is opened, the current in the inductor wishes to continue to flow in the same direction and with the same magnitude. Therefore the diode will turn on and the current will immediately flow into the filter capacitor and any connected load.

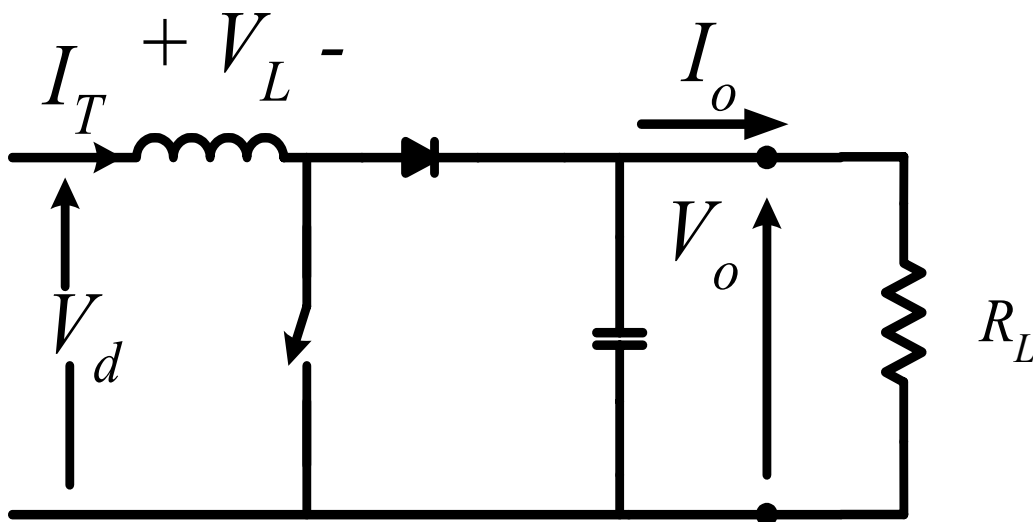


Fig.3.1 Step Up DC-DC converter (Boost converter)

The aim of this chapter is to express the system as a series of interconnected systems that interact to provide a collective response.

The expression of the project as sub-system blocks constitutes a significant portion of this text. By dividing the project into these sub system blocks the design can become a simpler project with each block relying on set assumptions and design goals. The goal of this approach is to design a system that can be altered with ease and can more importantly be tested on a per entity basis. This testing concept allows each system to have a greater reliability due to the high reliability of surrounding components. Thus prerequisite for each sub system module is justified. The system can be

simplified for design purposes by breaking down the system into a series of sub-systems connected together in a network configuration. Consider the block representation of the system below.

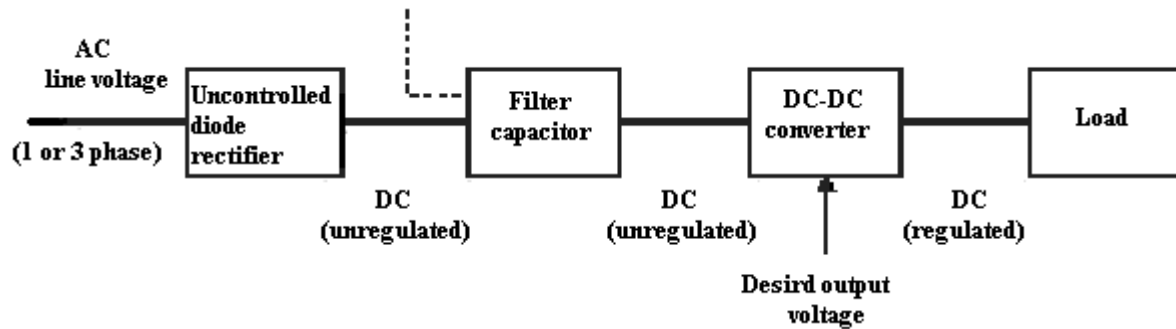


Fig.3.2 Block diagram of the structure of a typical DC-DC converter.

The system of a DC speed controller was separated into several components, which rely on each component around them for operation. This may be related to an object oriented design approach taken in software design.

The project was divided into sub-sequent parts, control circuit components and power circuit components.

Each of these component parts is related together to represent the entire system. This approach was also useful in regards to testing the various features of the system where the functionality of each block could be completed separately.

These sub-systems are the subject of analysis, design and implementation throughout the remainder of the chapters comprising this project composition.

### 3-2 Control Circuit Components

The control circuit components consist of the following parts:

#### 3-2-1 DC Power Supply

The most critical system with regard to the entire system is the power supply. If the power supply is not operational then the entire circuit is not operational. It could be said that the power supply is the stomach of the system and without energy the system would not operate. It is used to supply power to the integrated circuits (ICs) and for the analog circuits.

This division of the system supplies +15 V, -15 V, and 0 V to the entire system to operate all the integrated circuitry of the micro-controller unit. The following are some details of the power supply components:

## Transformer Connection

To convert the AC mains voltage to a useable voltage to then be filtered a transformer is required to step down the voltage rectifier bridge. The transformer connections to supply the regulators are as shown in Fig.3.3.

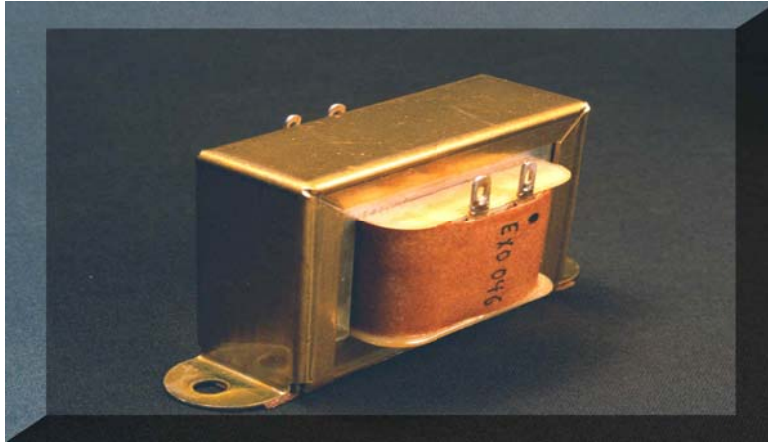


Fig.3.3 Transformer which we use it.

The transformer selected for this section was 240 V 30 VA tapped secondary transformer. The secondary taps selected to be used from the transformers were 0 V, 15 V, and 30 V, which were arranged to provide +15 V, 0 V and -15 V to the system. A 500 mA fuse was used with this transformer to provide a protection and safety device.

## Rectifier Circuit

The voltage output from the transformer is given as shown in Fig.3.4. But when the transformation through the rectifier bridge occurs, the output DC voltage is obtained from the following equation:

$$V_{dc1} = \frac{\sqrt{2} V_m}{\pi} = \frac{\sqrt{2} * 24 * \sqrt{2}}{\pi} = 15.2V \quad (3.1)$$

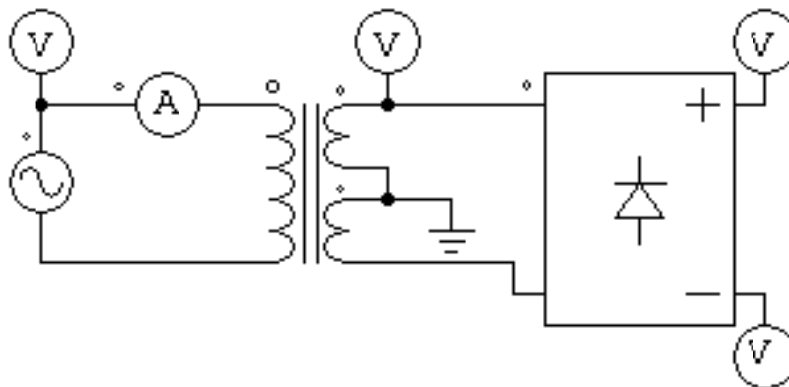


Fig.3.4 Transformer and rectifier connection.

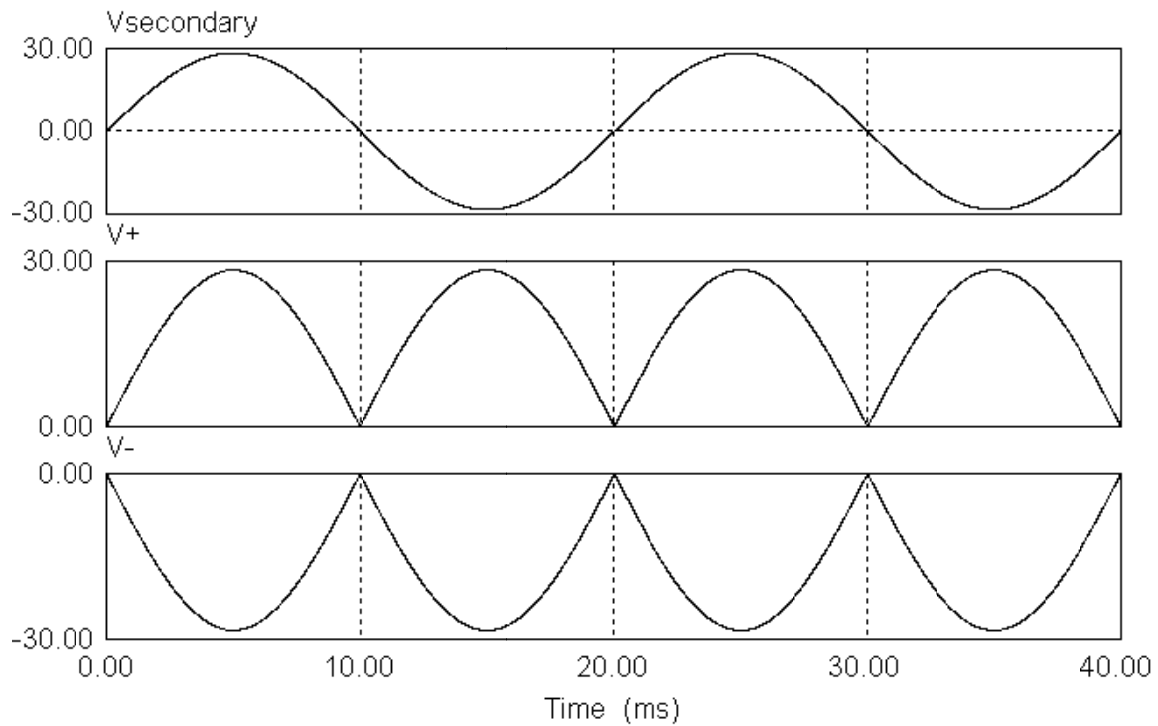
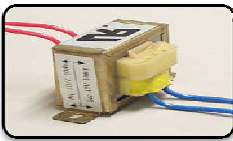


Fig.3.5 The output voltage for the previous connection.

The initial stage of this project was to prototype a Power Supply Module. LM7815 and LM7915 are used to supply +15 Volts and -15 Volts respectively. The expected total power consumption required by the circuits is approximately 10 Watts. All capacitors should be the highest quality, especially the output capacitor. The input capacitor is an easier-to-get size capacitor of 100 microfarads; I included the output capacitor of 10 microfarads to help eliminate any distortion when it is supplying the analog circuits. The component required:



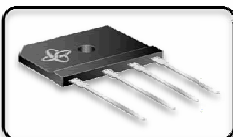
**Transformer 220/ 24-0-24**



**Two Regulator 7815 & 7915**



**Two capacitors 100uF & two capacitors 10uF**



**Bridge diode**

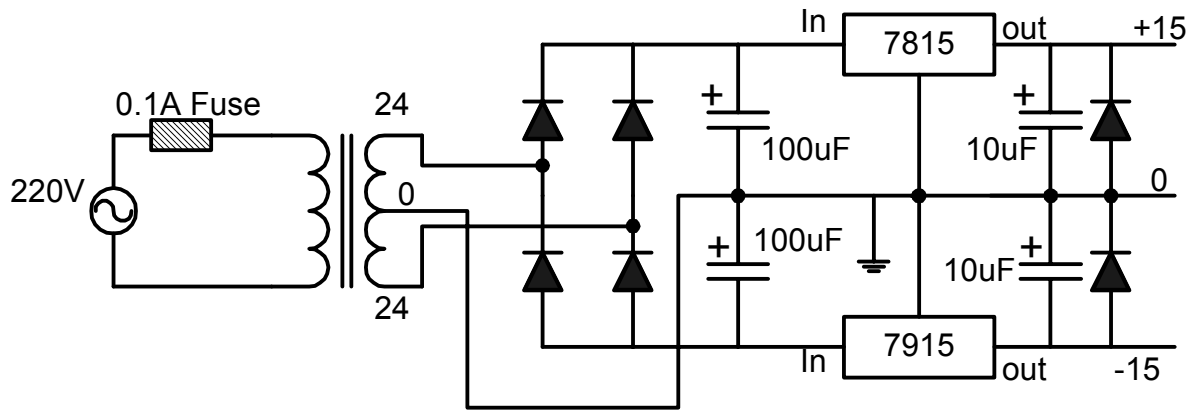


Fig.3.6 Schematic diagram of the power supply module.

### 3-2-2 Voltage Controlled Saw-tooth Oscillator and Comparator

The voltage controlled oscillator (VCO) is an oscillator whose frequency can be changed by a variable DC control voltage. One way to build a voltage controlled saw-tooth oscillator is with an op-amp integrator that uses a switching device (PUT) in parallel with the feedback capacitor to terminate each ramp at a prescribed level and effectively "rest" the circuit. Fig.3.7 shows the implementation of this circuit.

The PUT is a programmable unijunction transistor with an anode, a cathode and a gate terminal. The gate is always biased positively with respect to the cathode. When the anode voltage exceeds the gate voltage by approximately 0.7 V, the PUT turns on and acts as forward biased diode, when the anode voltage falls below this level, the PUT turns off. Also, the current must be above the holding value to maintain conduction. The frequency of the saw-tooth oscillator can be obtained from the following equation:

$$f_s = \frac{(R_2)V_{cc}}{R_1 + R_2} * \frac{1}{R_i C} \left( \frac{1}{V_P - 1} \right) \quad (3.2)$$

$$\text{Where } V_P = \frac{R_4}{R_3 + R_4} (V_{cc}) + 0.7 \quad (3.3)$$

$$\text{Then, } V_P = \frac{10}{6 + 10} (15) + 0.7 = 10.075 \text{ V} \quad (3.4)$$

Then the minimum switching frequency can be obtained when the input resistance is at its maximum value as following:

$$f_s - \min = \frac{(6)*15}{6 + 6} * \frac{1}{100 * 10^3 * 10 * 10^{-9}} \left( \frac{1}{8.2 - 1} \right) = 1042 \text{ Hz} \quad (3.5)$$

The maximum value can be obtained from the performance of the circuit. The sawtooth signal has to be compared using voltage comparator (see Fig.3.7) with variable control signal by us 100 k potentiometer. The output from comparator depends on the following logic.

If  $V_{control} > V_{sawtooth}$  the output voltage will be +15V and

If  $V_{control} < V_{sawtooth}$  the output voltage will be -15V

So, if we need the output voltage to be zero when  $V_{control} < V_{sawtooth}$  we can use diode at the output signal as shown in Fig.3.7. Therefore, with the diode connected at the output, the output from comparator depends on the following logic.

If  $V_{control} > V_{sawtooth}$  the output voltage will be +15V and,

If  $V_{control} < V_{sawtooth}$  the output voltage will be 0 V

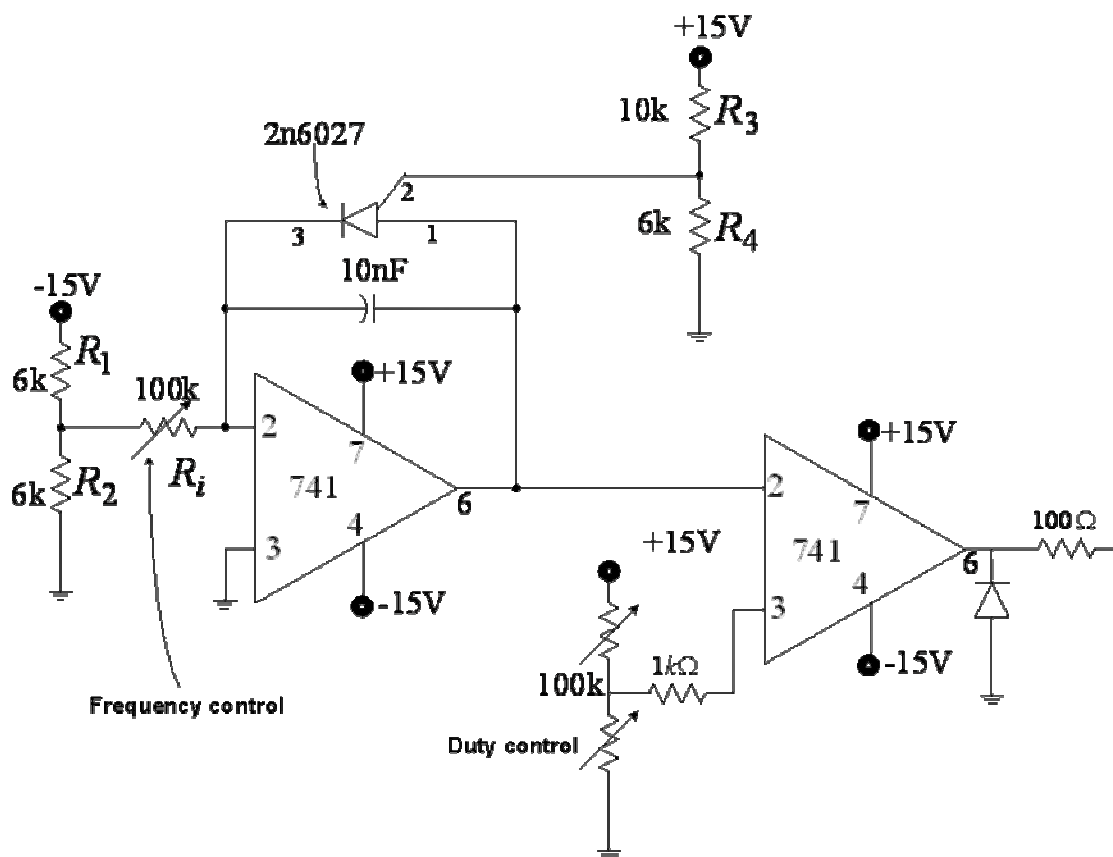


Fig.3.7 Voltage controlled saw-tooth oscillator and comparator circuit

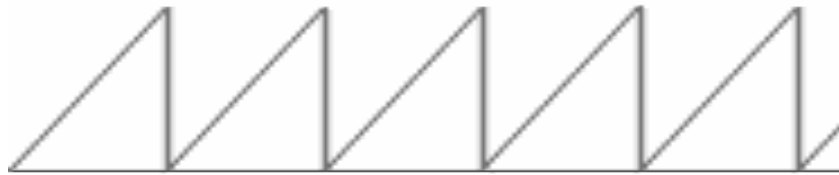


Fig.3.8 Sawtooth wave.

### 3-2-3 Comparator

Comparator is the second op-amp in control circuit, it compare between the sawtooth wave and a DC voltage at specified level we make control on the DC voltage by an potentiometer 100 kilo ohms it can make the output DC voltage from 10V to 15V the applied DC voltage at the 3<sup>rd</sup> terminal of the 741 IC (positive input).

The negative input is the sawtooth wave it is applied at the 2<sup>nd</sup> terminal of the 741 IC as we see in the Fig.3.7.

The output of the comparator is +15 voltage when the control voltage (DC voltage) is greater than the sawtooth wave it be -15 when the control voltage is less than the sawtooth wave as we see in the middle waveform of Fig.3.8.

At the output of the comparator we connect a suitable diode to remove –Ve component at the output of the comparator to make it +Ve only.

Resistance connected between the output and the MOSFET gate to protect the gate of the MOSFET and make it surly open or closed.

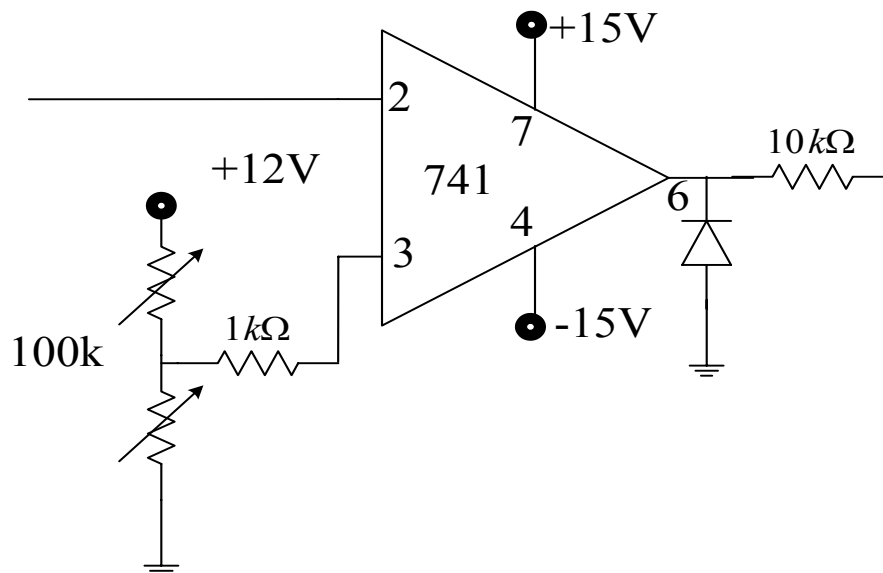


Fig.3.9 The comparator circuit.



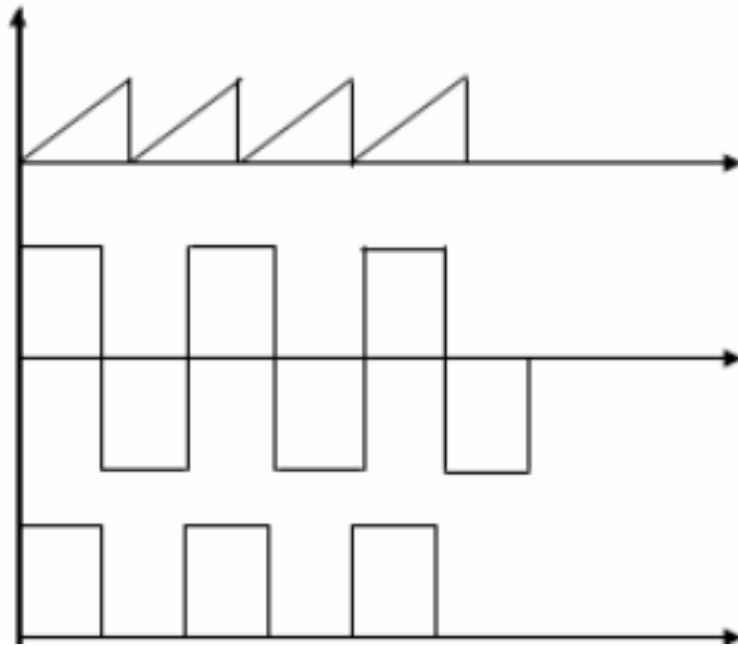
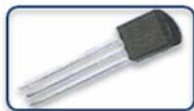
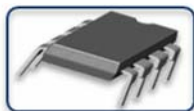


Fig.3.10 The output of voltage of the comparator circuit.

Voltage controlled saw-tooth circuit components:-



**PUT 2n6027**



**Two OP-amp 741**



**Diode**



**Ceramic Capacitor 10nF**



**Two Potentiometer 100k**



**Resistors**

### 3-3 Power Circuit:

Power circuits feed the DC motor with a voltage between 10V and 80V as a variable DC voltage. The DC Motor speed is proportional with the applied voltage on it. So we design our power supply to vary the input voltage of the DC motor to change its speed. Power Circuit (see Fig.3.11) is consisting of the following components:

#### Power Transformer

We choose a suitable step down transformer with the following specification:

Primary voltage is 220V sinusoidal AC

Secondary voltage is 12V sinusoidal AC

It has VA equal 25 VA

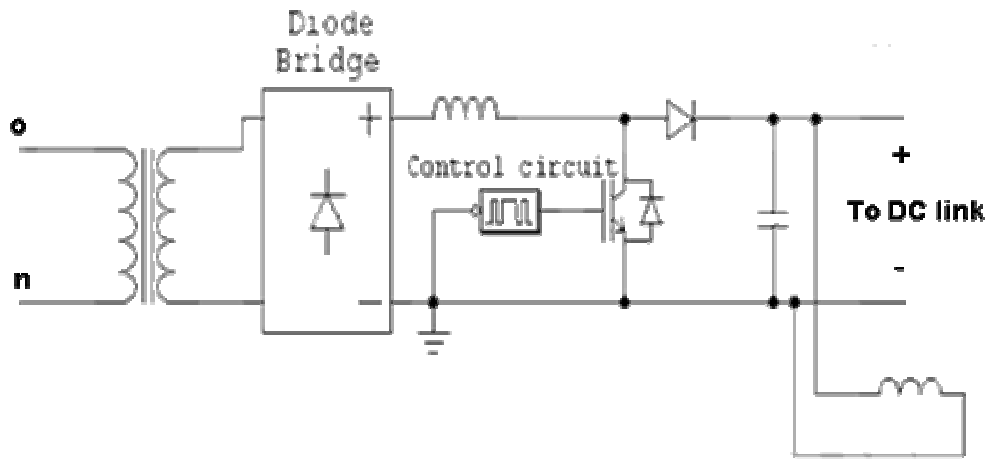


Fig 3.11 Power circuit of boost converter.

Bridge or 4 suitable diodes

The bridge has the following specification:

It can operate with the full load current (10A) without over heated. The output of the bridge can be obtained by the following equation:

$$V_{dc} = \frac{1}{\pi} \int_0^{\pi} V_m \sin \omega t \, d\omega t = \frac{2V_m}{\pi} = \frac{2 \cdot 12 \cdot \sqrt{2}}{\pi} = 10.8V \quad (3.6)$$

## Inductance

We made our inductance with the following specifications.

Ferromagnetic core, Diameter of the wire is suitable for the full load current

## Switch (MOSFET or IGBT)

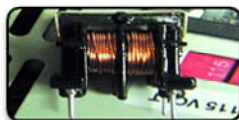
MOSFET plays a significant role in controlling the applied voltage on the DC Motor. It's Gate triggered by the output of the controlling circuit. We can recognize that the MOSFET is used on this design in place of IGBT switch.

## Smoothing Capacitor

We use this capacitance to make the output nearing the pure DC voltage. We choose this capacitance suitable and can be withstand with the applied voltage (80 V). Power circuit component required:-



**Transformer**



**Inductance**



**MOSFET**



**Capacitor 470uF(250V)**



**High current diode**



**bridge diode**

### 3-4 Isolating Circuit:

We will implement this circuit to make isolation between the ground of supply and the ground of switch, the component required are:



Transformer 220/ 18-0-18



Optocoupler 4N32



Regulator 7815



Two capacitors 10uF



Bridge diode

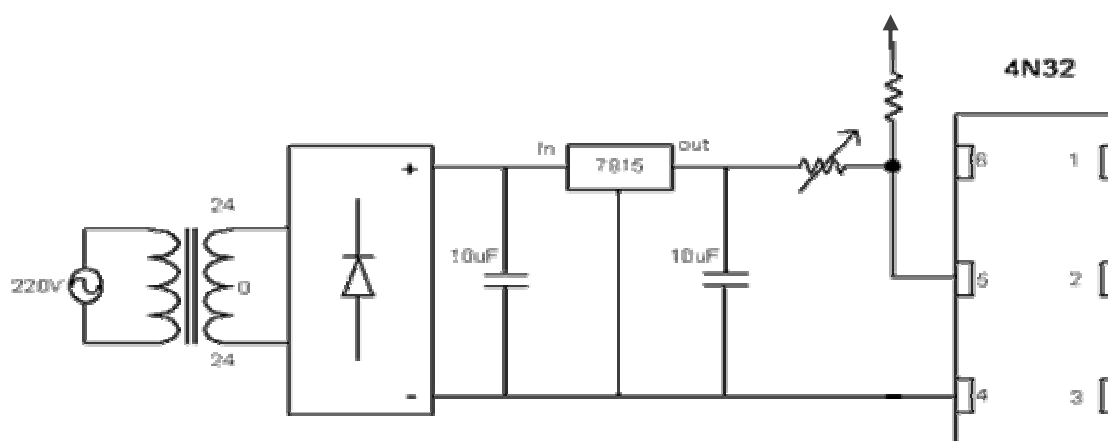


Fig.3.12 Schematic diagram of the isolating circuit.

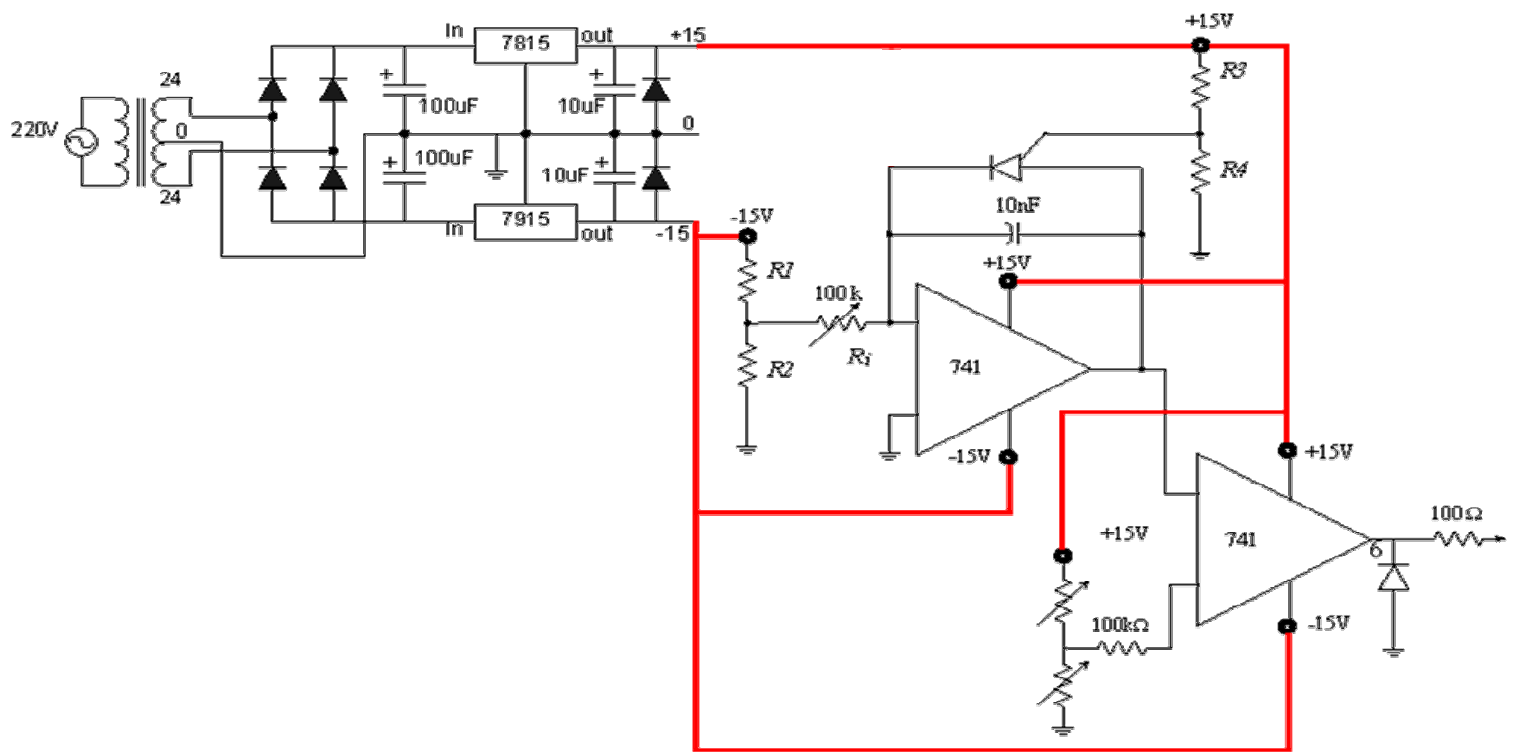


Fig.3.13 Schematic diagram of control circuit

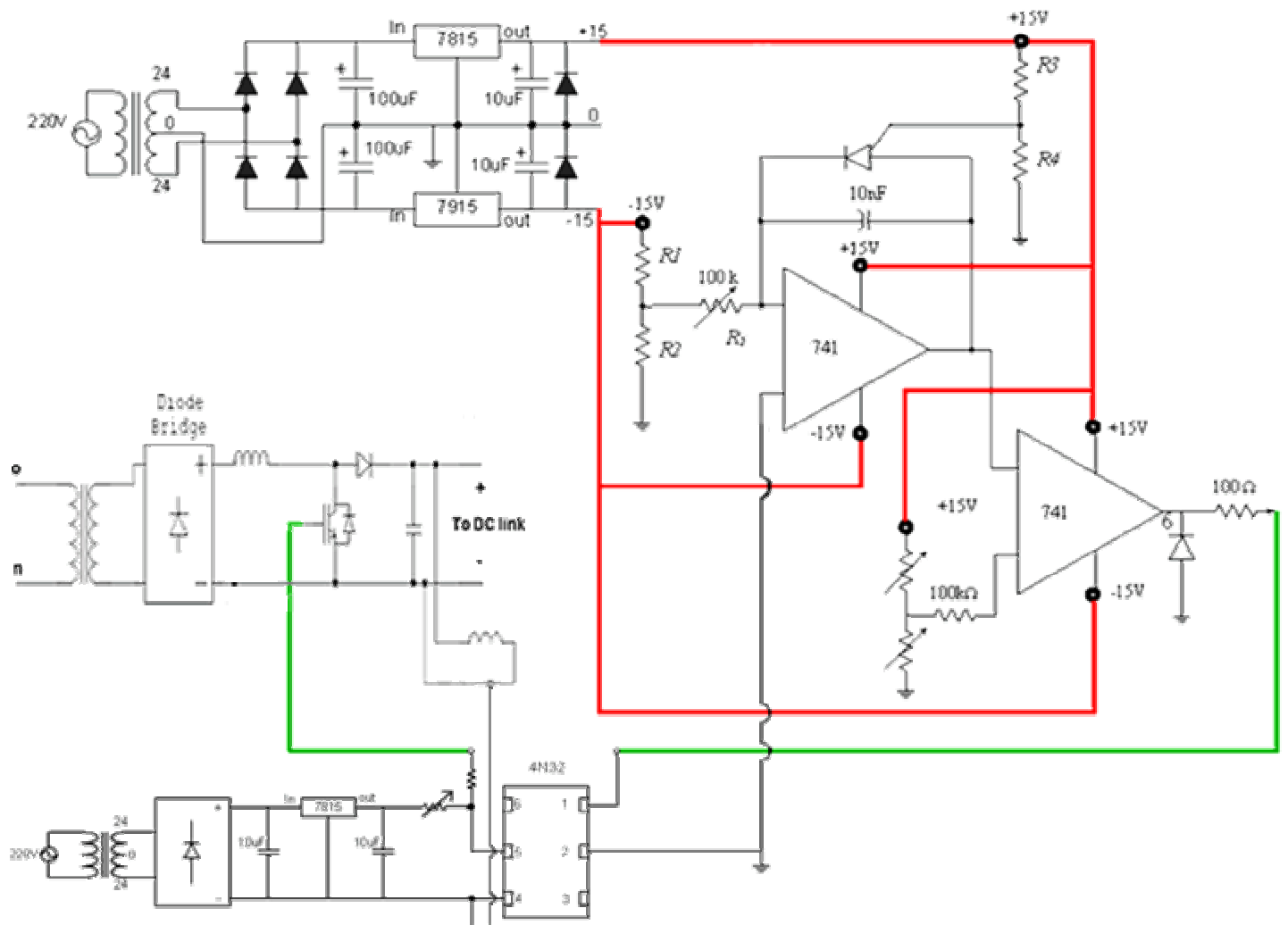


Fig.3.14 Schematic diagram of connection between power circuit and control circuit after isolation

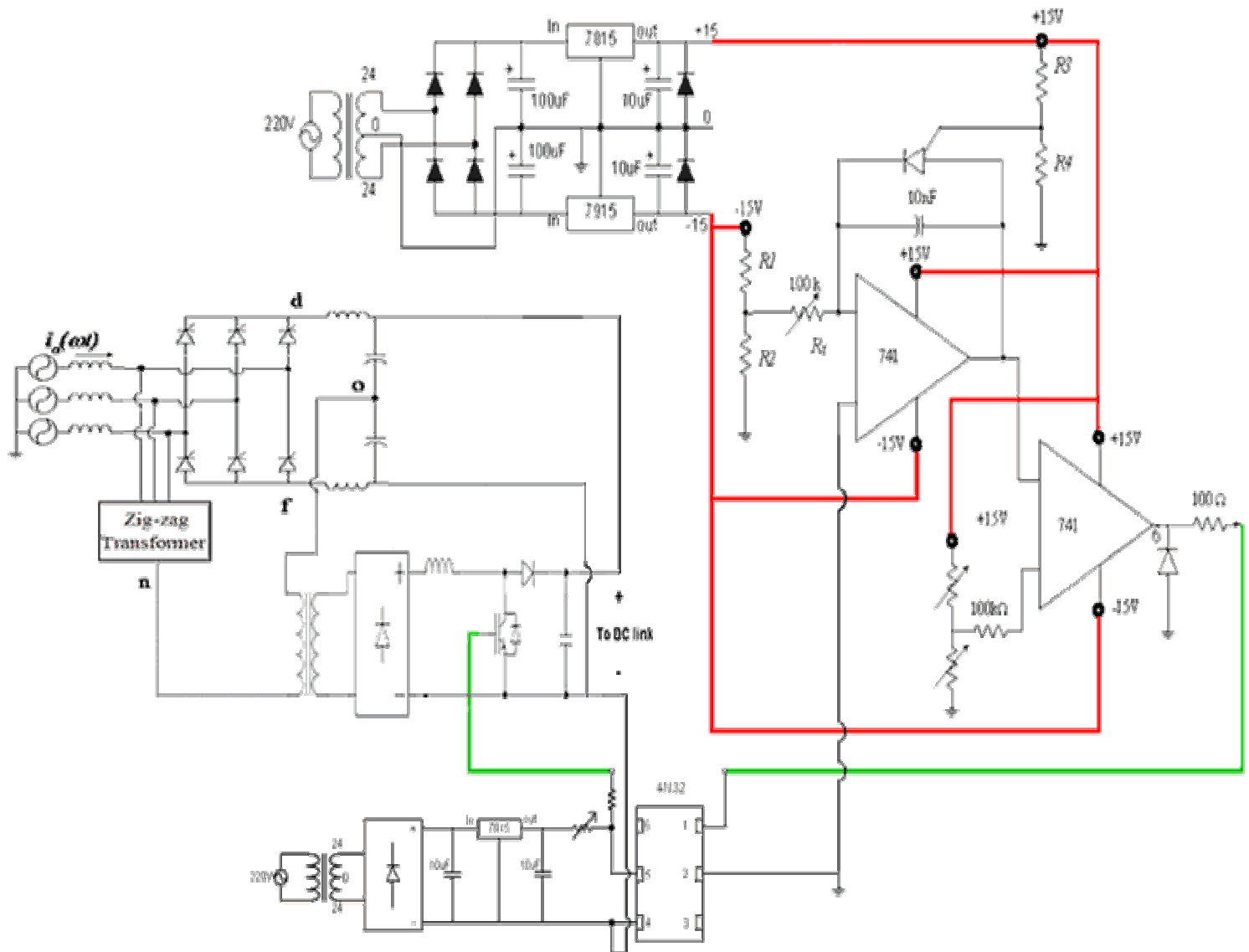


Fig.3.15 The injection technique by using boost converter

### 3-5 Simulation and Experimental Results:

The simulation performed for 110 V line-to-line voltages and 220  $\mu$ F, DC-link capacitor. Fig.3.16 (a) and (b) shows the simulation, experimental result for utility line current  $i_a(\omega t)$  along with phase  $a$  voltage for zero injection current at  $\alpha = 20^\circ$ . Fig.3.16 (b) shows the FFT components of phase  $a$  current. It is clear from this figure that the line current contains high harmonics especially from 5<sup>th</sup> and 7<sup>th</sup> components.

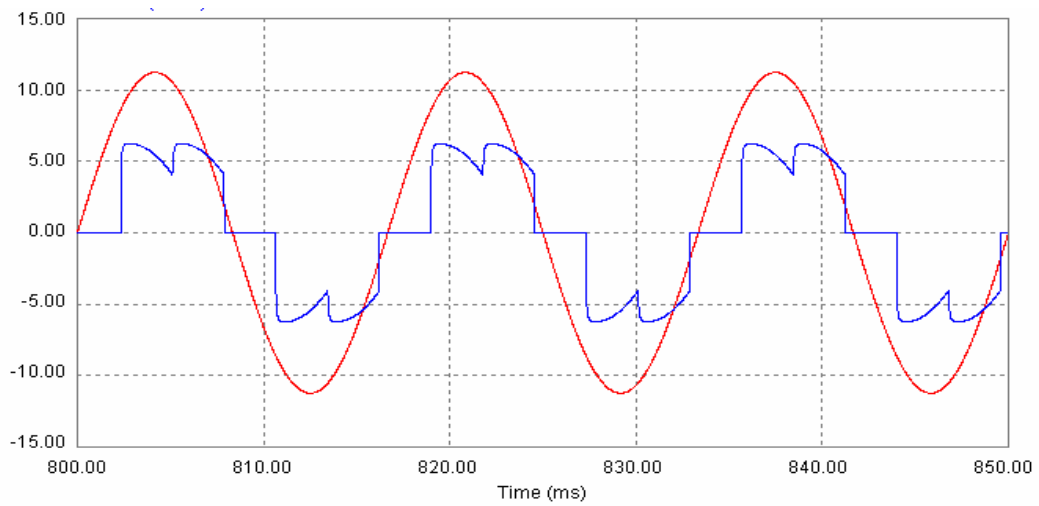
Fig.3.17 (a) and (b) shows the simulation, experimental result for utility line current  $i_a(\omega t)$  along with phase  $a$  voltage for optimum injection current,  $I_f$  at  $\alpha = 20^\circ$ . Fig.3.17 (b) shows the FFT components of phase  $a$  current. It is clear from this figure that the line current become very near to sine-wave with very low THD which prove the superiority of the third harmonic injection technique.

Fig.3.18 (a) and (b) shows the simulation and experimental results for the voltage  $V_{dn}$  along with phase  $a$  voltage. Fig.3.18 (c) shows the FFT components for the voltage  $V_{dn}$  at  $\alpha = 20^\circ$ . It is clear from this figure that this voltage contains high 3rd harmonic component. This component is used to drive the third harmonic injection current.

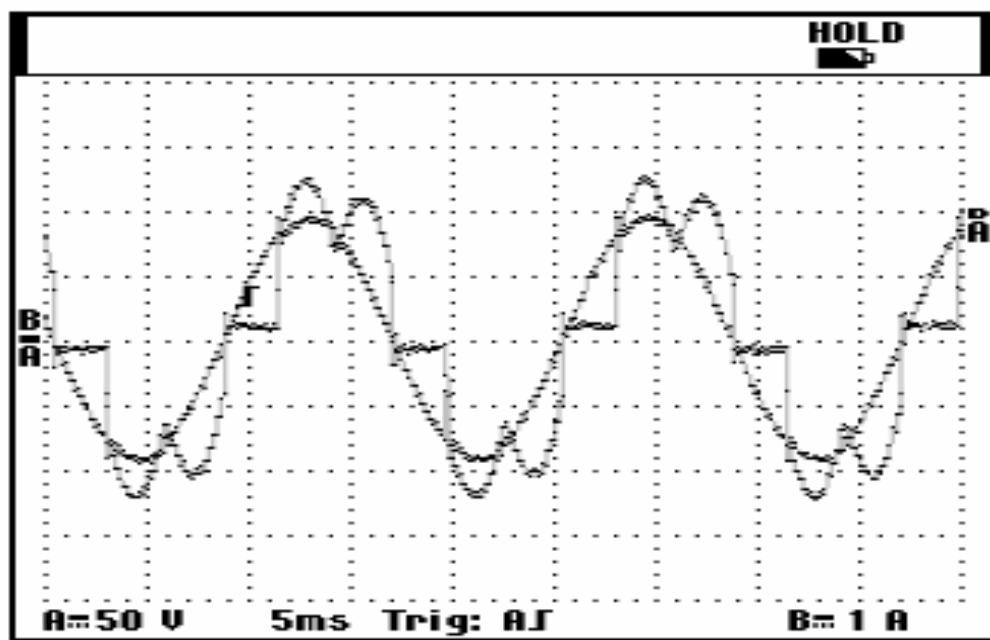
Fig.3.19 (a) and (b) shows the simulation and experimental results for the voltage  $V_{fn}$  along with phase  $a$  voltage. Fig.3.19 (c) shows the FFT components for the voltage  $V_{fn}$  at  $\alpha = 20^\circ$ . It is clear from this figure that this voltage contains high 3rd harmonic component. This component is used to drive the third harmonic injection current.

Fig.3.20 (a) and (b) shows the simulation result for  $V_a$  and injection current  $I_f$  at  $\alpha = 20^\circ$ , Fig.3.20 (c) shows the FFT components of the 3<sup>rd</sup> harmonic injection current.

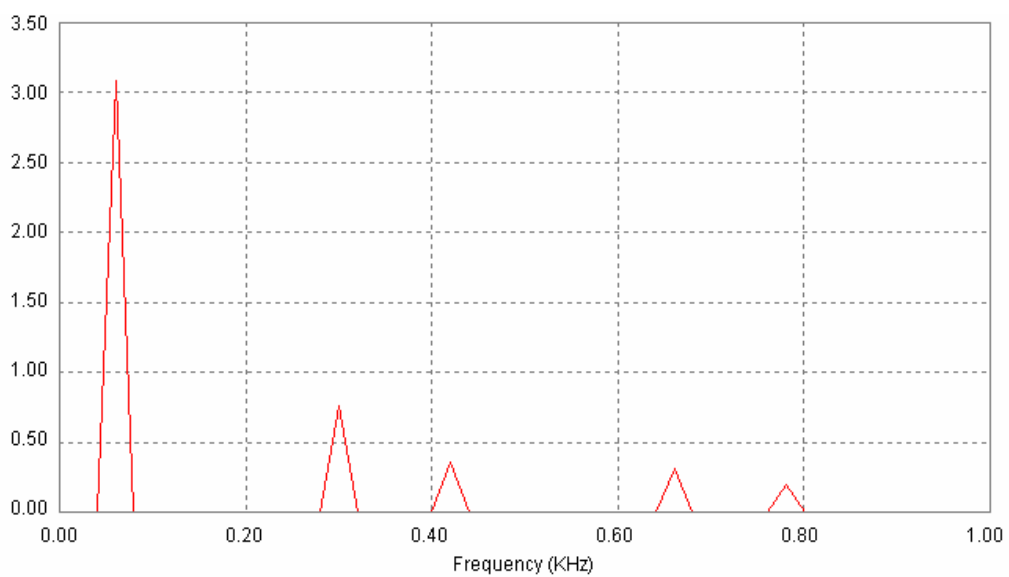
Fig.3.21 (a) (b) shows the simulation and experimental result line current  $i_a(\omega t)$  and injection current  $I_f$  at  $\alpha = 20^\circ$ .



(a) Simulation result.



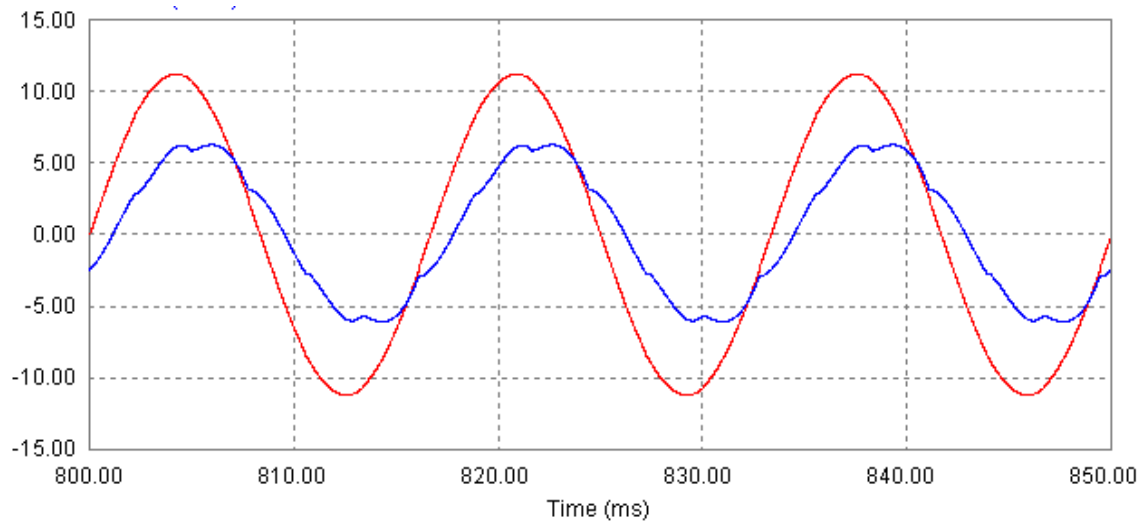
(b) Experimental Results



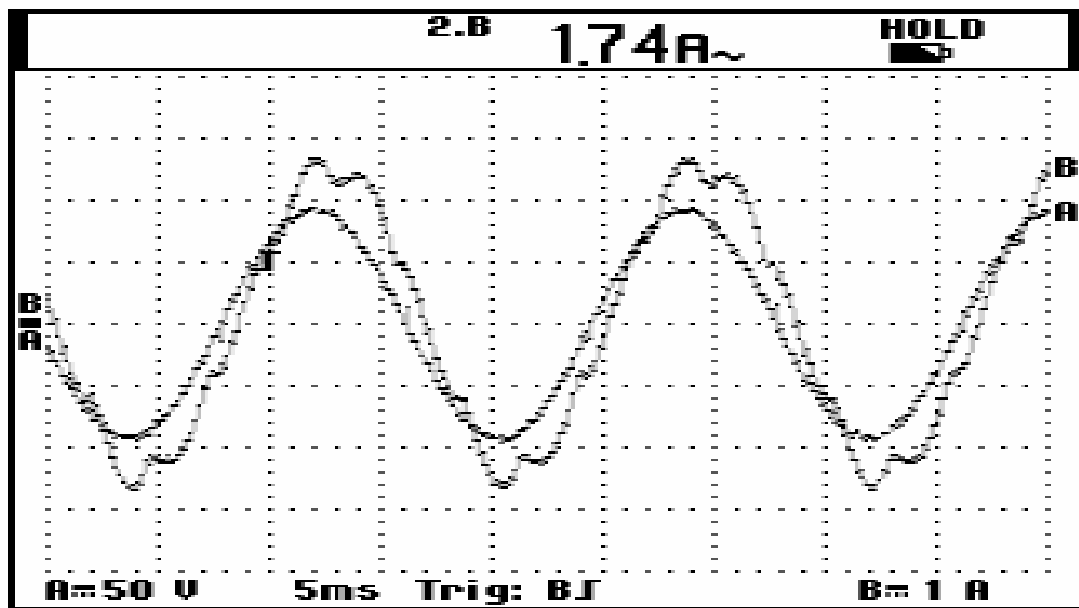
(c) FFT of  $I_a$

Fig.3.16 The utility line current at  $\alpha = 20$  along with phase a voltage and its FFT components without injection.

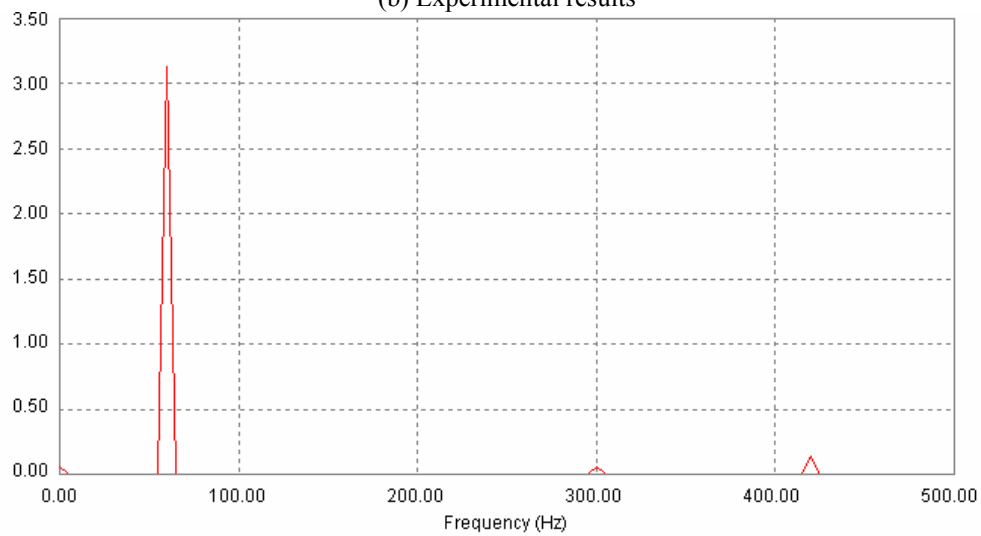




(a) Simulation result

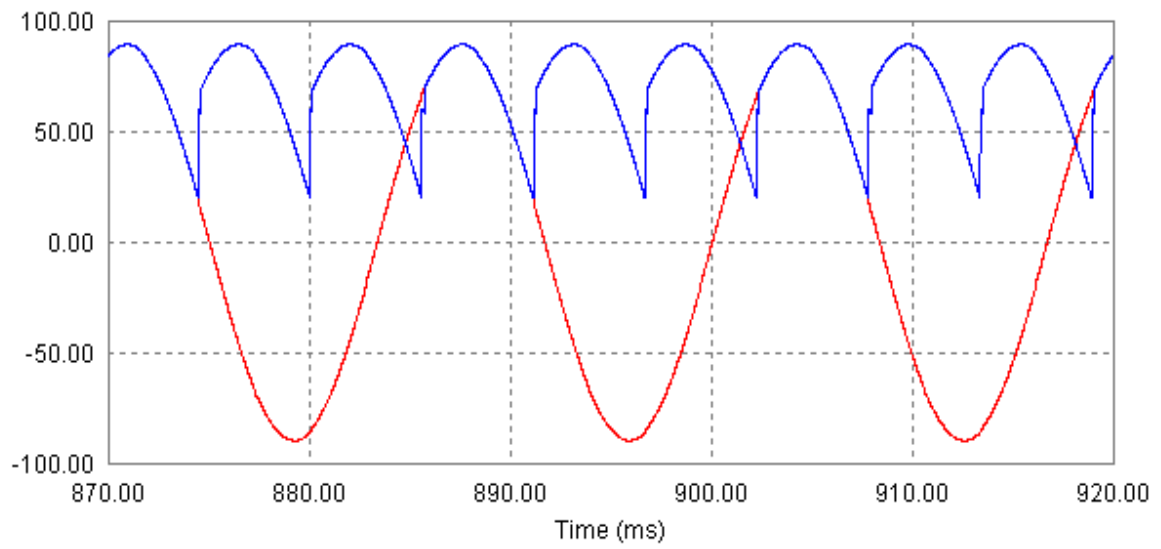


(b) Experimental results

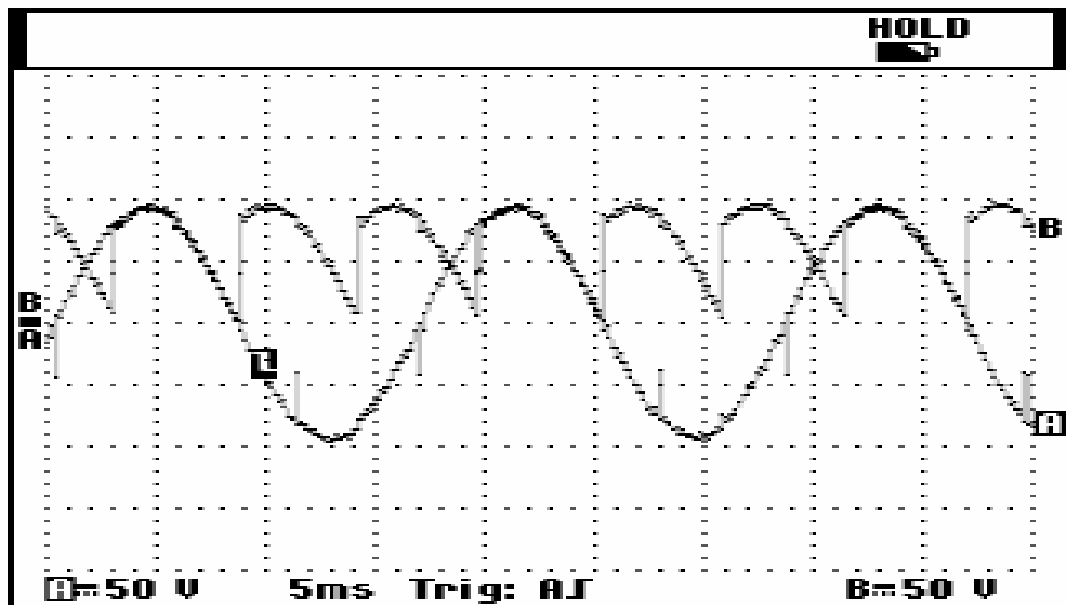


(c) FFT of  $I_a$

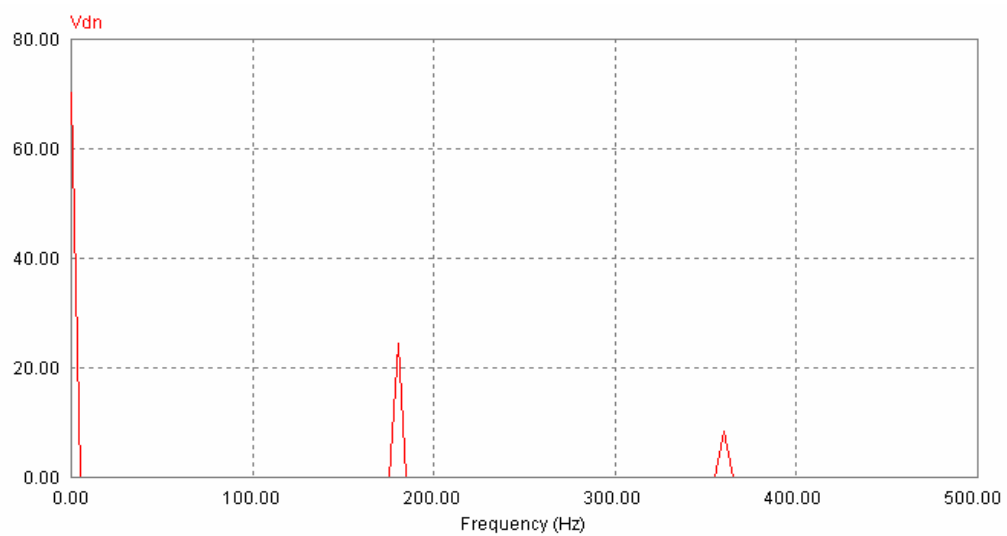
Fig.3.17 The utility line current at  $\alpha = 20$  along with phase a voltage and its FFT components with optimum injection current.



(a): Simulation results

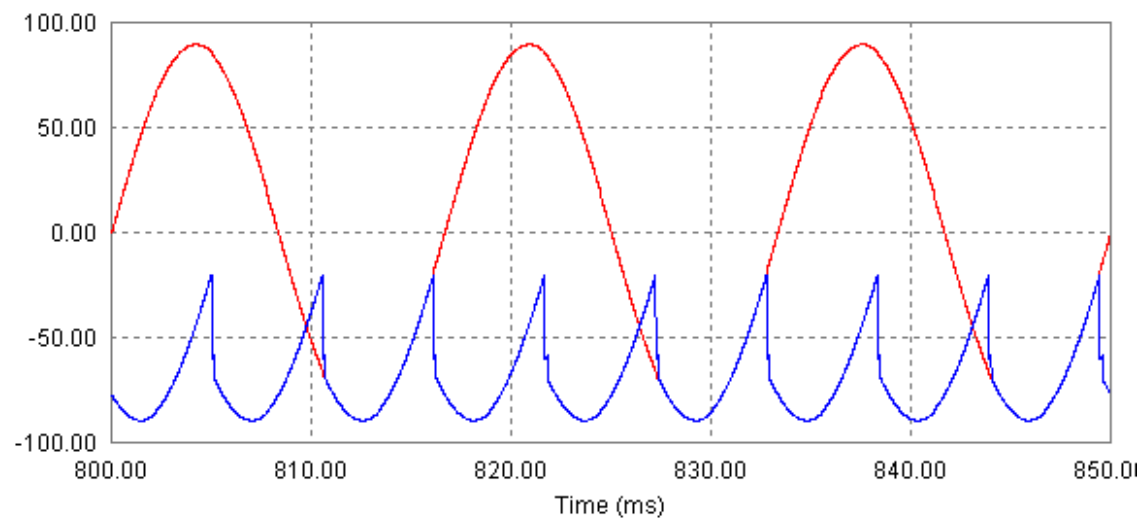


(b): Experimental result.

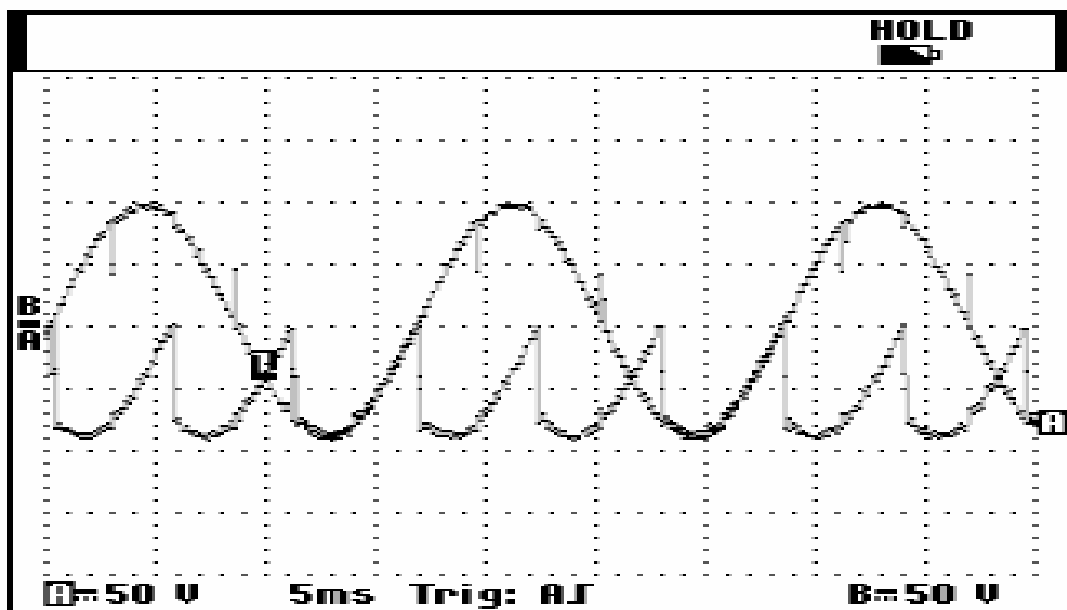


(c) FFT for  $V_{dn}$  at  $\alpha = 20^\circ$ .

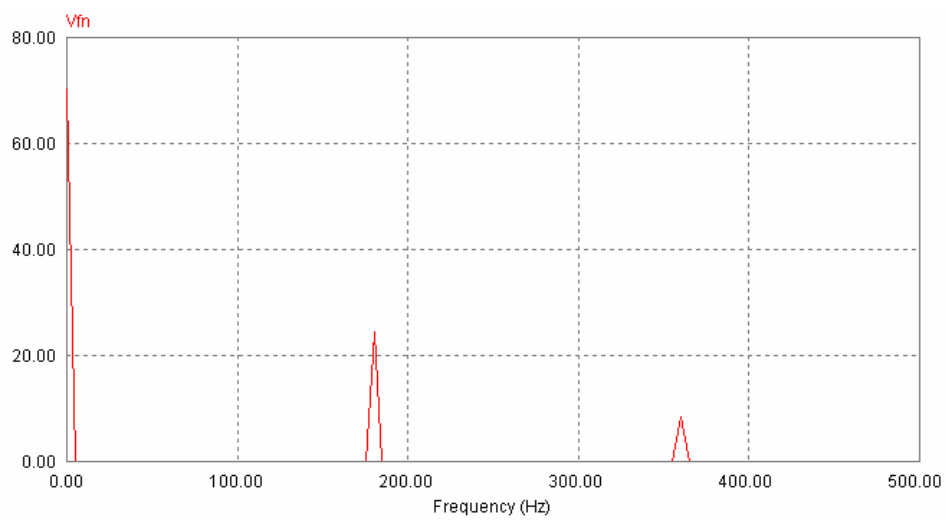
Fig.3.18 The voltage  $V_{dn}$  and its FFT components.



(a): Simulation results

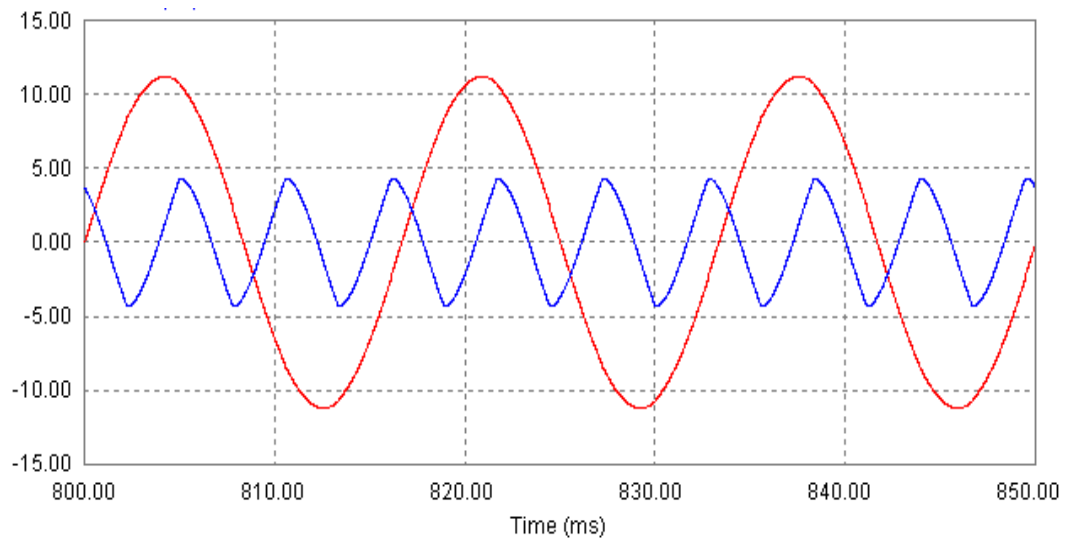


(b): Experimental result.

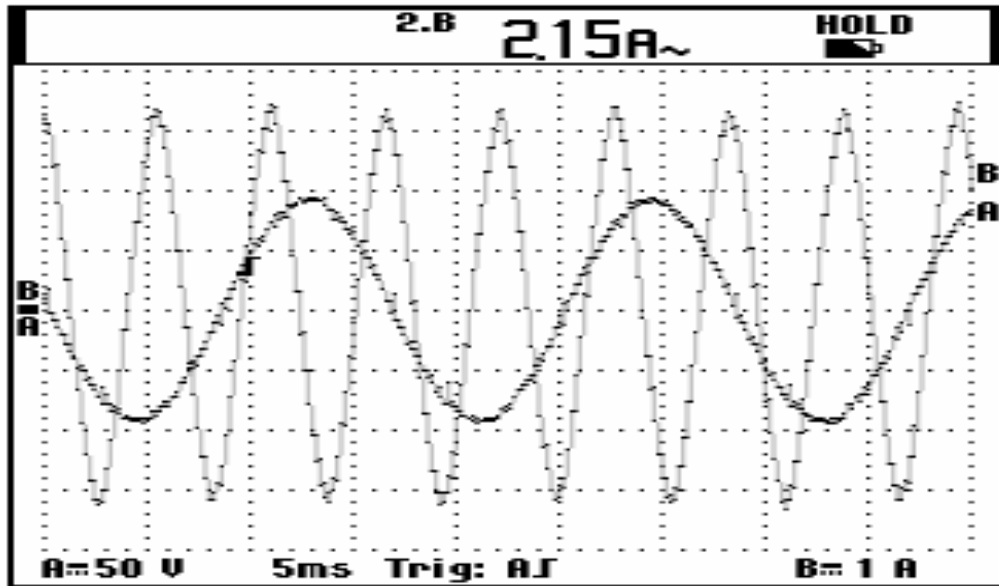


(c) FFT for  $V_{dn}$  at  $\alpha=20^\circ$ .

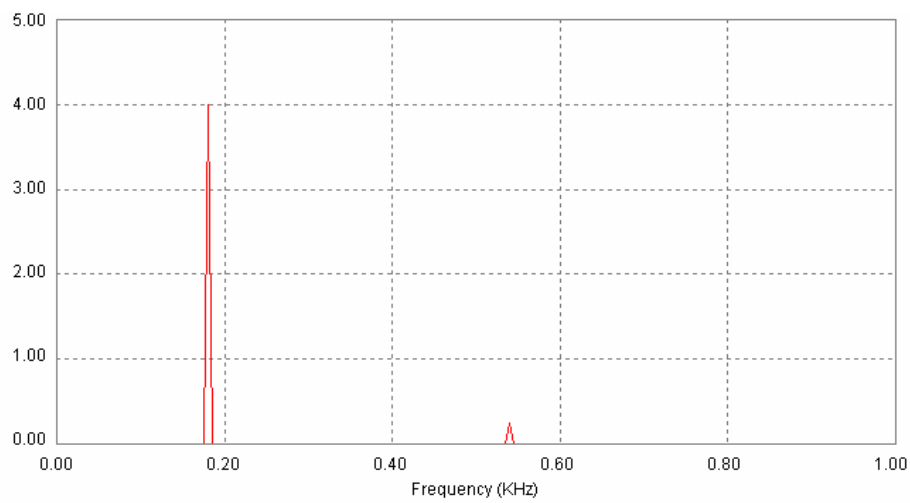
Fig.3.19 The voltage  $V_{fn}$  and its FFT components.



(a) Simulation Result

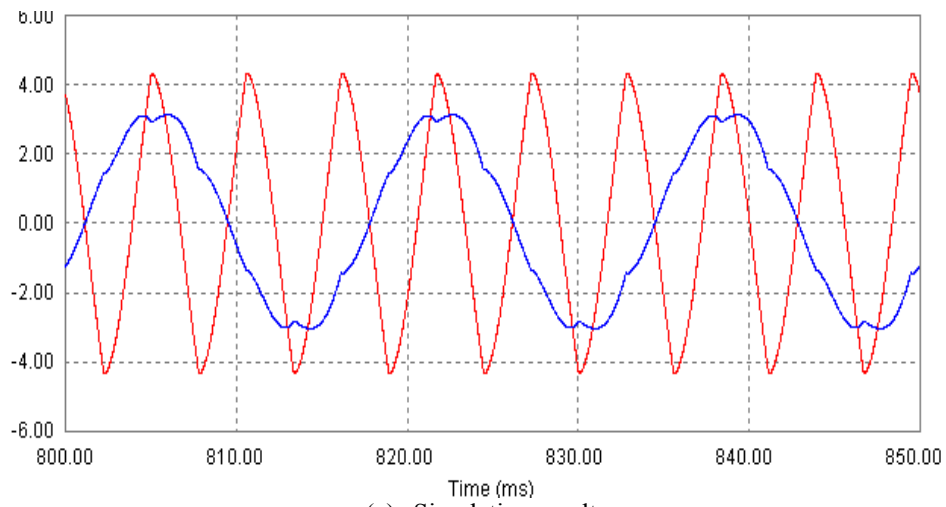


(b) Experimental Results

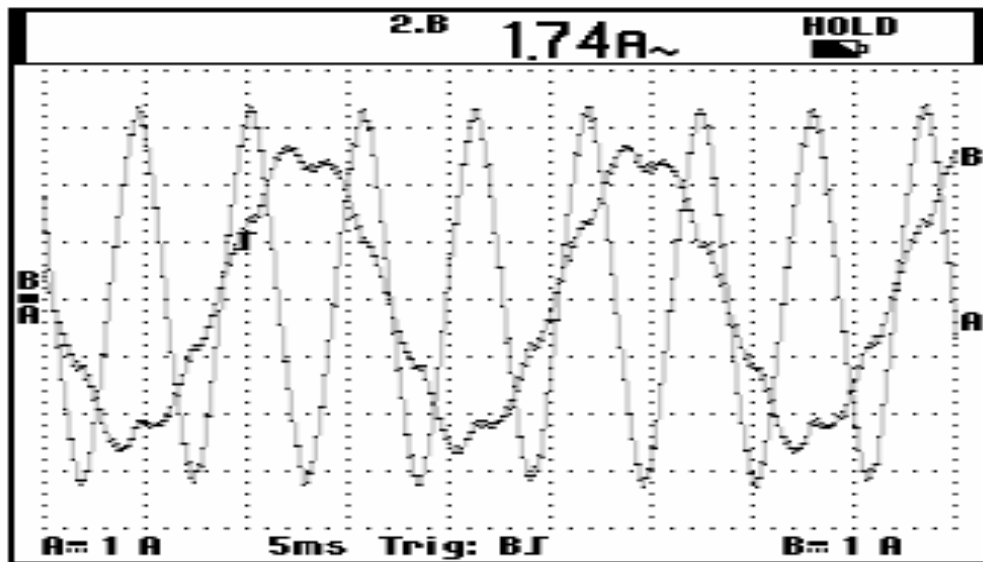


(c) FFT of  $I_f$

Fig.3.20 The voltage  $V_a$  and injection current  $I_f$  at  $\alpha = 20^\circ$



(a) Simulation result



(b) Experimental result.

Fig.3.21 The simulation and experimental result of line current  $i_a(\omega t)$  and injection current  $I_f$  at  $\alpha = 20^\circ$ .

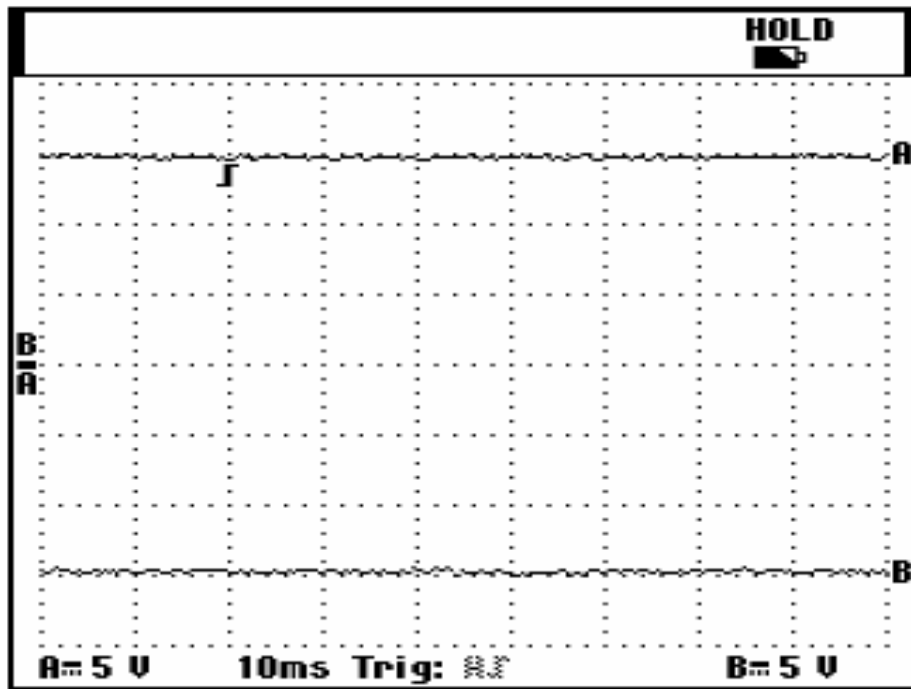


Fig.3.22 output of two regulator

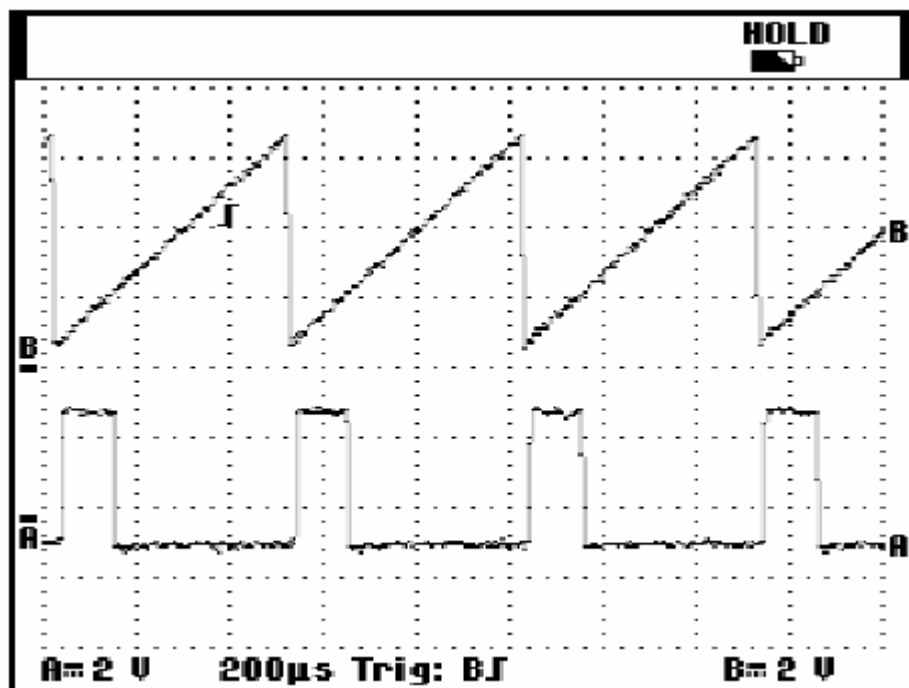


Fig.3.23 Sawtooth and pulse

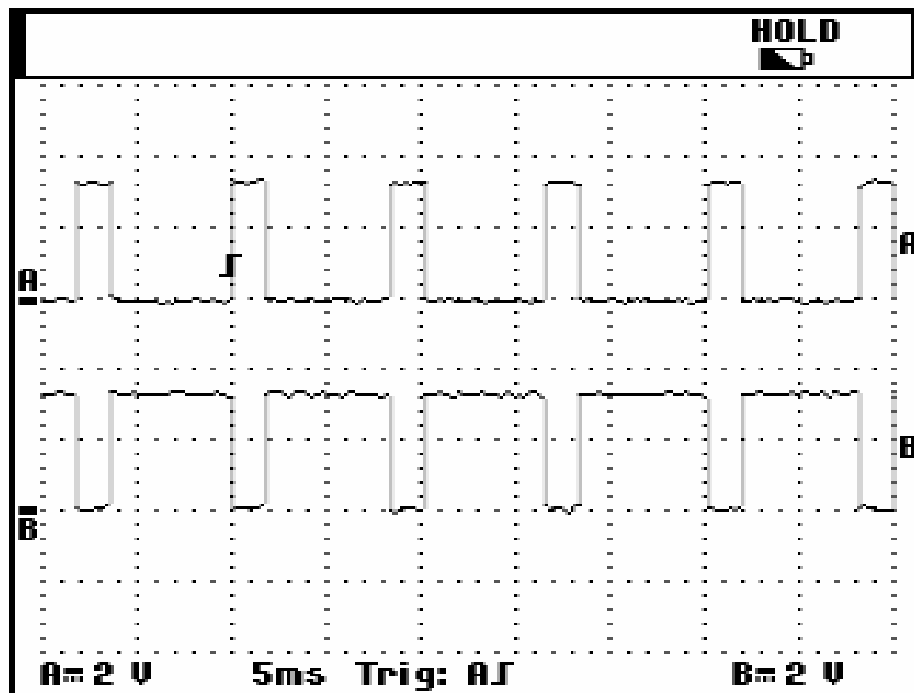


Fig.3.24 input and output of pulse

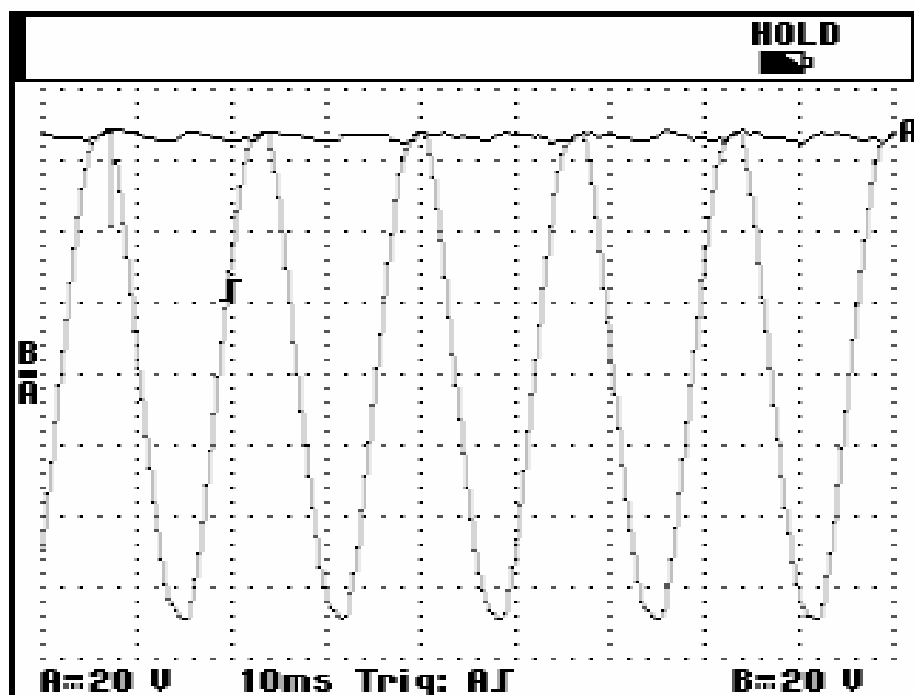


Fig.3.25 input and output of control bridge

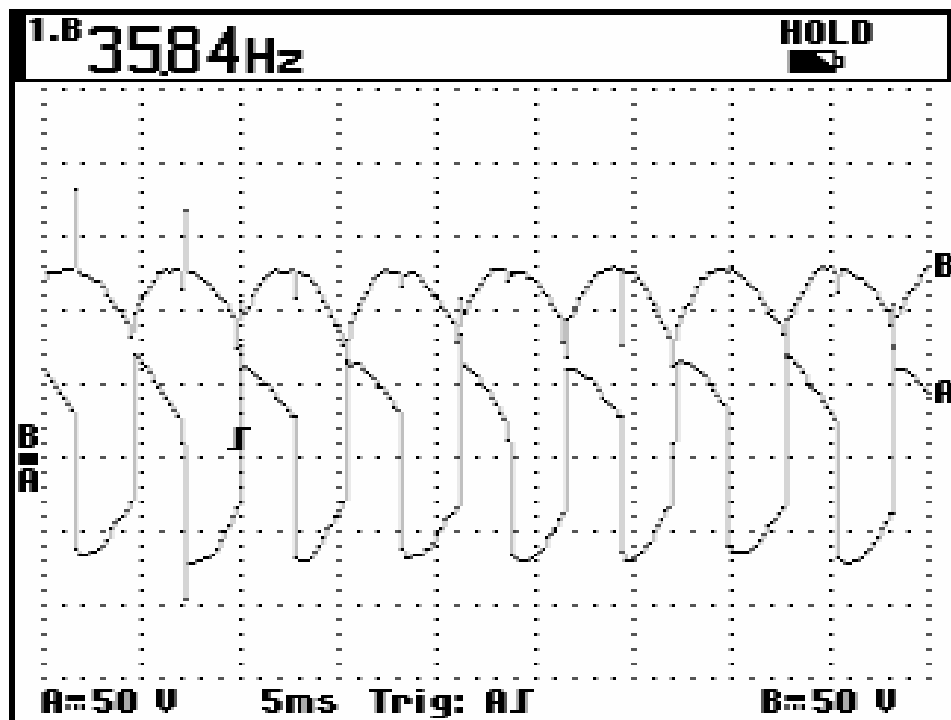


Fig.3.26 input and output of bridge for power circuit

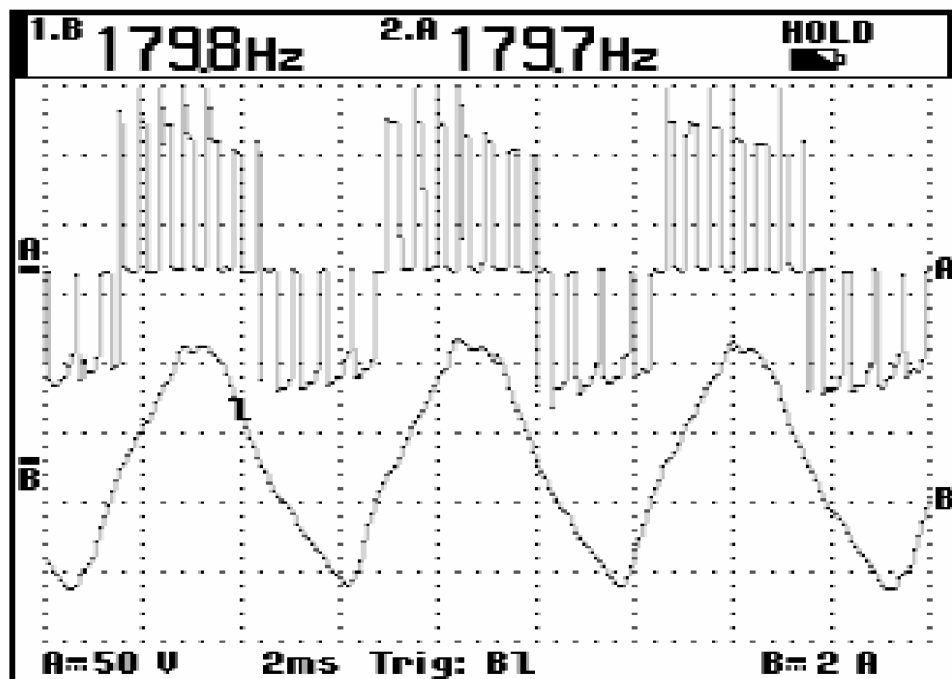


Fig.3.27 input boost voltage AC and If



### 3.6 Conclusions:

An approach to reduce harmonic based on circulating third harmonic current in the DC-link back to the utility line currents to reduce utility line current harmonics. A new shape is computed from analysis to achieve clean power characteristics with zero THD in utility line current. The computed shape is very near to sinusoidal third harmonic current. The optimal rms value of injection current is found about 1.2 times the DC current. The angle of injection current is varied with the firing angle of the converter. For this reason a variable R-L-C circuit has been used to control the amplitude and angle of the injected current. The resistance in the 3<sup>rd</sup> harmonic injection path has been replaced by boost converter to return the power that was dissipated in the resistor back to DC link to increase the efficiency of the system. The proposed technique eliminates the high power interface transformer with only 25% zig/zag transformer. Mathematical and simulation results verified the concepts. Experimental results were provided from 110V supply agrees with mathematical and simulation results. The proposed approach shows high performance and eliminates most problems associated with utility interface of SCR converters.